Article

ZOOTAXA

Two new species of geckos of the genus *Phyllopezus* Peters, 1878 (Squamata: Gekkota: Phyllodactylidae) from northeastern Brazil

MARCOS J. M. DUBEUX[1,2,3,*], UBIRATAN GONÇALVES[2,3], CRISTIANE N. S. PALMEIRA[2,4], PEDRO M. S. NUNES[1], JOSÉ CASSIMIRO[5], TONY GAMBLE[6,7,8], FERNANDA P. WERNECK[9], MIGUEL T. RODRIGUES[5] & TAMÍ MOTT[2,3]

[1]*Programa de Pós-Graduação em Biologia Animal, Departamento de Zoologia, Centro de Biociências, Universidade Federal de Pernambuco, Avenida Professor Moraes Rego, 1235, Cidade Universitária, 50670-901, Recife, Pernambuco, Brasil.*
 https://orcid.org/0000-0002-2635-9703

[2]*Setor de Herpetologia, Museu de História Natural, Universidade Federal de Alagoas, Avenida Amazonas, S/N, Prado, 57010-060, Maceió, Alagoas, Brasil.*

[3]*Setor de Biodiversidade, Instituto de Ciências Biológicas e da Saúde, Universidade Federal de Alagoas, Av. Lourival Melo Mota, S/N, Tabuleiro do Martins, 57072-900, Maceió, Alagoas, Brasil.*
 https://orcid.org/0000-0003-2076-9063
 https://orcid.org/0000-0002-5896-4780

[4]*Programa de Pós-Graduação em Desenvolvimento e Meio Ambiente, Departamento de Botânica e Zoologia, Centro de Biociências, Universidade Federal do Rio Grande do Norte, Campus Universitário, Lagoa Nova, 59078-900, Natal, Rio Grande do Norte, Brasil.*
 https://orcid.org/0000-0002-7085-3741

[5]*Departamento de Zoologia, Instituto de Biociências, Universidade de São Paulo, Rua do Matão, Travessa 14, 05508-090, São Paulo, São Paulo, Brasil.*
 https://orcid.org/0000-0003-3958-9919

[6]*Department of Biological Sciences, Marquette University, Milwaukee, WI 53233, USA.*

[7]*Milwaukee Public Museum, Milwaukee, WI 53233, USA.*

[8]*Bell Museum of Natural History, University of Minnesota, St Paul, MN 55113, USA.*
 https://orcid.org/0000-0002-0204-8003

[9]*Programa de Coleções Científicas Biológicas, Coordenação de Biodiversidade, Instituto Nacional de Pesquisas da Amazônia, Av. André Araújo, 2936, Petrópolis, 69067-375, Manaus, Amazonas, Brasil.*
 https://orcid.org/0000-0002-8779-2607

[*]*Corresponding author.* *marcosdubeux.bio@gmail.com;* *https://orcid.org/0000-0003-3049-1720*

Abstract

We describe two new species of Brazilian geckos of the genus *Phyllopezus* based on morphological and molecular data. The first species is currently known from a relictual Cerrado enclave—"*campos rupestres*", in the mountains of the Serra do Espinhaço in the state of Bahia. The second species is known from northeastern Atlantic Forest and transitional areas with Caatinga biome in the state of Alagoas. The two new species are sister taxa and together are the sister clade to the remaining species in the *Phyllopezus pollicaris* species complex. These new species can be morphologically distinguished from their congeners by meristic and morphometric characters, in addition to color pattern and genetic differentiation.

Key words: Cryptic diversity; integrative taxonomy; lizard; morphological data; molecular phylogeny

Introduction

The genus *Phyllopezus* Peters, 1878 includes saxicolous and arboreal lizards distributed predominantly in the dry-open biomes of South America (Caatinga, Cerrado, and Chaco; Werneck *et al.* 2012; Cacciali *et al.* 2018). The genus is morphologically diagnosed by skin with small granular scales with equidistant larger tubercles, tail with small rhomboid scales, a single series of undivided lamellae under the base of the digits and, by the two distal phalanges in all digits, narrowing towards the claw (Vanzolini 1953; Vanzolini *et al.* 1980; Rodrigues 1986). The monophyly of the genus is supported by molecular data, including mitochondrial (16S rRNA, Cytb and ND2) and nuclear (*e.g.*, RAG1, RAG2, C-MOS and ACM4) genes (Gamble *et al.* 2012; Werneck *et al.* 2012; Cacciali *et al.* 2018).

Currently *Phyllopezus* is composed of six formally described species: *P. heuteri* Cacciali, Lotzkat, Gamble & Köhler, 2018 (restricted to the Chaco biome in the Cordillera de Los Altos mountain range, Paraguay; Cacciali *et al.* 2018), *P. lutzae* (Loveridge, 1941) (restricted to the Atlantic Forest biome of northeastern Brazil, with distribution extending from the state of Paraíba to Bahia; Albuquerque *et al.* 2019), *P. maranjonensis* Koch, Venegas & Böhme, 2006 (distributed in the dry forests of the upper Marañon basin, Peru; Koch *et al.* 2006), *P. periosus* Rodrigues, 1986 (distributed in the northern Caatinga biome of states of Ceará to Pernambuco), *P. przewalskii* Koslowsky, 1895 (distributed in the Chaco biome of Paraguay, Bolivia and north of Argentina and in the Cerrado biome, below the Central Brazilian Shield, in the states of Mato Grosso and Mato Grosso do Sul (Condez *et al.* 2021), and *P. pollicaris* (Spix, 1825) (widely distributed in the Caatinga and Cerrado biomes and entering the Atlantic Forest in the eastern coast of Brazil; Condez *et al.* 2021), which includes an extremely high hidden diversity (*e.g.* Pellegrino *et al.* 1997; Gamble *et al.* 2012) resulting in multiple evolutionary lineages (Gamble *et al.* 2012; Werneck *et al.* 2012) that still await formal descriptions.

Werneck *et al.* (2012), using molecular data, recovered eight lineages associated to *P. pollicaris* sensu lato in the Caatinga, Cerrado, and Chaco biomes (Clades I–VIII), and treated them as candidate species. In that work, the authors resurrected the nominal taxon *P. przewalskii* to accommodate populations belonging to Clade V, rendering *P. pollicaris* paraphyletic. Later, Cacciali *et al.* (2018) described a new lineage (*P. heuteri*) related to *P. przewalskii*, which had not been included in previous studies. Combined with high genetic diversity (Gamble *et al.* 2012; Werneck *et al.* 2012) and the presence of multiple reciprocally monophyletic groups there is a clear need of taxonomic studies to delimit and describe the cryptic diversity within the genus.

Herein we use an integrative approach, including molecular data and external morphology to describe two new species of *Phyllopezus* (currently assigned to the *P. pollicaris* complex) from northeastern Brazil. We also define the *P. pollicaris* complex as the clade comprised of *P. pollicaris* sensu lato, *P. przewalskii*, and *P. heuteri*.

Material and methods

Analyzed specimens. We examined 146 specimens of *Phyllopezus* including representatives of all nominal taxa occurring in the Northeast region of Brazil (*P. lutzae*, *P. periosus*, and *P. pollicaris*; Fig. 1; Appendix I). All *P. pollicaris* specimens analyzed for external morphology come from localities represented in the molecular datasets used in recent phylogenies (*i.e.*, Gamble *et al.* 2012; Werneck *et al.* 2012). Specimens are deposited in the following herpetological collections: Coleção Herpetológica do Museu de História Natural da Universidade Federal de Alagoas (MHN-UFAL), Coleção Herpetológica da Universidade Federal da Paraíba (CHUFPB), Coleção Herpetológica da Universidade Federal de Pernambuco (CHUFPE), Coleção Herpetológica da Universidade Federal do Rio Grande do Norte (UFRN) and Coleção Herpetológica do Museu de Zoologia da Universidade de São Paulo (MZUSP). Paralectotypes of *Phyllopezus pollicaris* (ZSM 165/0/1–2) were examined through photographs (available in Cacciali *et al.* [2018]).

Phylogenetic inference and genetic distance analyses. *Phyllopezus pollicaris* Clade I [sensu Werneck *et al.* (2012); specimens from municipality of Mucugê, state of Bahia, hereafter treated as *Phyllopezus* sp.1] have been previously considered as a candidate species (Gamble *et al.* 2012; Werneck *et al.* 2012; Cacciali *et al.* 2018). When analyzing the morphology of this candidate species, we noticed its similarity with some specimens occurring in the state of Alagoas, which although morphologically different from *P. pollicaris* sensu stricto, had never been included in a molecular study. We complemented the existing dataset of partial 16S rRNA sequences with representatives of three different locations for this population of Alagoas state [hereafter treated as *Phyllopezus* sp.2; see Appendix II for GenBank accession numbers, vouchers, and localities; note that representatives of *P. pollicaris* Clades II and III of Werneck *et al.* (2012) were not included due to the lack of 16S rRNA sequences].

DNA was extracted using phenol/chloroform protocol (Sambrook & Russel 2001). Subsequently, a fragment of the 16S rRNA mitochondrial gene was amplified through polymerase chain reaction (PCR), using the primers 16Sar-L and 16Sbr-H (Palumbi *et al.* 2002). Reactions consisted of 25 µl solution containing 12.5 µl of Master Mix PCR Buffer Promega® with 0.4 mM of each dNTP and 3 mM of MgCl2, 8.4 µl of nuclease-free water, 0.5 µl of Taq DNA polymerase Invitrogen® (5U/µl), 0.8 µl of each primer (10pmol) plus 2 µl of DNA template (20–100 ng/µl). Samples were amplified with: (1) initial denaturation at 94 °C for 90 sec followed by 35 cycles of denaturation at 94 °C for 45 sec, (2) annealing at 48 °C for 60 sec, and (3) extending at 72 °C for 60 sec. Samples were purified using

isopropanol and sent to be unidirectional sequenced using Sanger method at the Laboratório Central da Universidade Federal de Pernambuco (LABCEN), municipality of Recife, Pernambuco state, Brazil.

Sequences were aligned with other 45 sequences representative of all *Phyllopezus* clades (including two sequences of *Phyllopezus* sp.1; Appendix II) available on GenBank using MAFFT software v.7.310 with default parameters (Katoh & Standley 2013). Genetic distances within and between species and among clades recognized by Werneck *et al.* (2012) were then estimated using Kimura 2-parameters evolutionary models (K2P; Kimura 1980) and p-distance (p-D) with complete deletion of gaps, implemented in software MEGA X (Kumar *et al.* 2018).

The choice of the best evolutionary model for the character matrix was performed in PartitionFinder v.2.1.1 (Lanfear *et al.* 2012) using the Bayesian Information Criterion (BIC) and default settings. Bayesian analysis was performed in MrBayes software v.3.2 (Ronquist *et al.* 2012). The phylogenetic analysis consisted of two independent runs of 10 million generations each, being evaluated every 1,000 generations. The first 25% of trees were discarded as burn-in; the majority consensus tree was visualized using the program FigTree software v.1.3.1. Nodes with posterior probability above 0.95 were considered having high support. *Phyllodactylus xanti* Cope, 1863 was used for rooting the tree following Gamble *et al.* (2012).
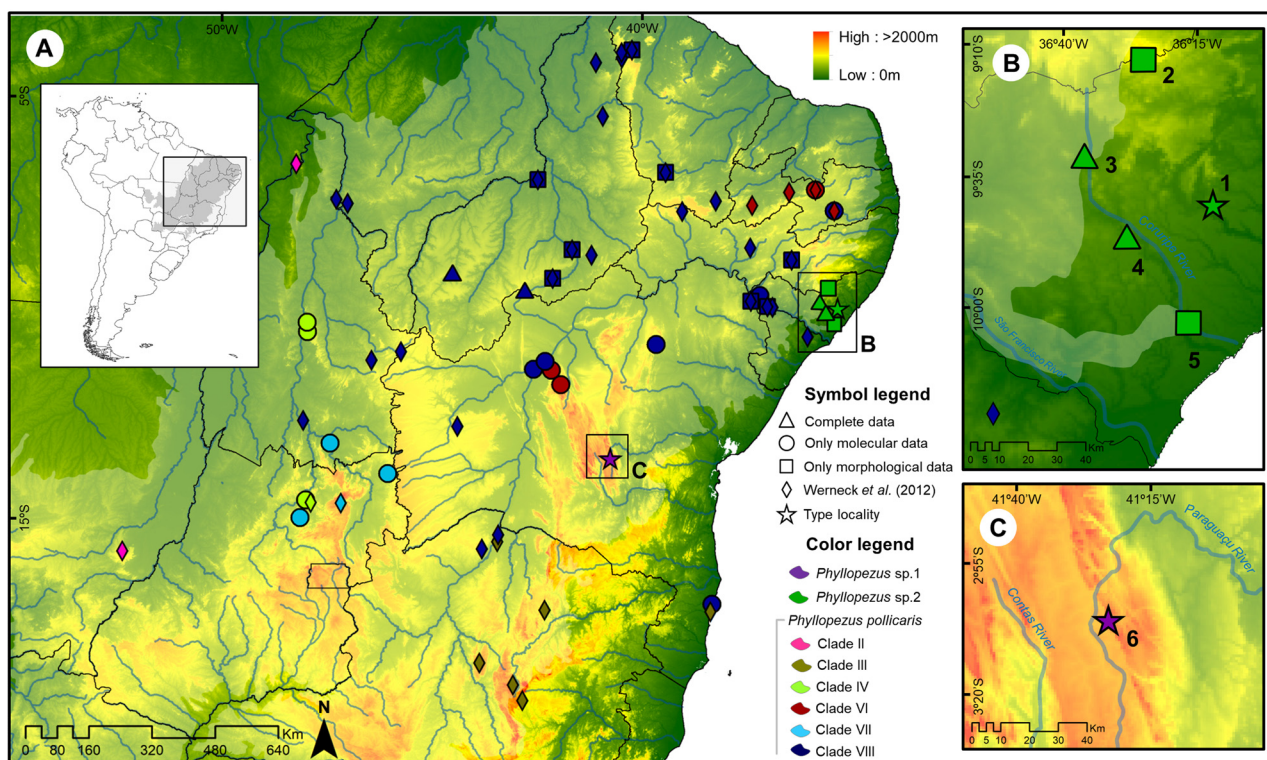

FIGURE 1. Geographic distribution of genetic and morphological vouchers of *Phyllopezus pollicaris* complex in northeastern Brazil. (A) *Phyllopezus pollicaris* clades (following Werneck *et al.* [2012]) and new samples analyzed in this study; (B) expanded view of the known distribution of *Phyllopezus* sp.2 in the state of Alagoas, Brazil; (C) expanded view of the known distribution of *Phyllopezus* sp.1 in the state of Bahia, Brazil. Numbers near the points correspond to the municipalities of (1) Boca da Mata, (2) Quebrangulo, (3) Igaci, (4) Limoeiro de Anadia and (5) Coruripe, state of Alagoas, and (6) Mucugê, state of Bahia, Brazil. Stars indicate type localities (with available morphological and molecular data) of *Phyllopezus* sp.1 (purple) and *Phyllopezus* sp.2 (green). Locations indicated with diamond denote samples of Werneck *et al.* (2012) not included in this study due to the absence of 16S rRNA data. Transparent white area [gray in the inset South America map in (A)] corresponds to Brazilian dry-open biomes. Inset map: South America.

Species delimitation analyses. Four different methods of single locus species delimitation were performed using the aligned 16S rRNA data (excluding external groups). (1) We calculated a cutoff point for probable intraspecific divergence, specifically for our data set, using the Local Minima function of the Species Identity and Evolution in R package (SPIDER; Brown *et al.* 2012) implemented in the R Studio software v.1.2.1 (R Core Team 2020). This analysis is based on the concept of a barcode gap, and species identification is not provided *a priori*. When the analysis detects a drop in the density of genetic distances, a possible transition between intra and

interspecific distance values is suggested. (2) We also performed an analysis of Automatic Barcode Gap Discovery (ABGD; Puillandre *et al.* 2011) implemented on the ABGD online platform (https://bioinfo.mnhn.fr/abi/public/abgd/), which is based on the general genetic divergences between sequences of the matrix, using values from a series of previous intraspecific divergences. For this analysis, sites with gaps were excluded, resulting in a matrix of 347 base pairs. Previous values for minimum and maximum intraspecific divergence were defined based on the results of Local Minima, and we also tested for values of interspecific divergence found between species already recognized in the genus (Gamble *et al.* 2012; Cacciali *et al.* 2018), and among gekkotan sister species (Rocha *et al.* 2009; Fujita *et al.* 2010). Values between 0.001 and 1.5 of relative gap were tested. (3) To delimit species based on the topology recovered, an analysis of Bayesian implementation of the Poisson Tree Process (bPTP; Zhang *et al.* 2013) was performed. This model uses a rooted phylogenetic tree to model speciation or branching events in terms of the number of substitutions. The analysis was performed on the PTP web server (https://species.h-its.org/ptp/) using default settings and clusters with support above 0.95 were indicated in the tree. (4) Finally, the Bayesian implementation of the Generalized Mixed Yule Coalescent model (bGMYC; Pons *et al.* 2006) was conducted. This model uses different topologies to model and to identify likely transition points between coalescence events and cladogenesis of alleles, incorporating phylogenetic uncertainties through a Bayesian extension (Reid & Carstens 2012). The topologies were obtained from a random selection of 100 trees resulting from a Bayesian inference implemented in the BEAST software v.1.8.4 (Suchard *et al.* 2018) using the GTR+Γ+I model (Suchard *et al.* 2018) in three independent analyses of 20 million generations each (sampling every 2 x 10^3) and 20% of initial burn-in. The bGMYC analysis was performed in the R Studio software for 100,000 generations with a burn-in of 90,000 and a dilution interval of 100 samples. A cut-off point for the probability of recognition of genetic clusters of 50% was adopted. To maximize the confidence of inferences (based on a single marker), we focus on species/lineages congruently retrieved/delimited by all methods as they can potentially be independent, but complementary.

External morphology. Measurements and scale counts were taken under a stereomicroscope. Measurements follow Rodrigues (1986), Cassimiro & Rodrigues (2009), and Sturaro *et al.* (2018), and were taken using a digital caliper to the nearest 0.1 mm (in right side of specimens whenever possible): snout-vent length (SVL, from tip of snout to cloacal opening), distance between limbs (DBL, from axilla to groin), tail base width (TBW, taken at the base of the tail just posterior to the cloaca), head length (HL, from tip of snout to anterior margin of ear-opening), head width (HW, on the widest part of head), head depth (HD, on the highest part of head), snout length (SL, from tip of snout to anterior margin of eye), nares-snout distance (NSD, from tip of snout to anterior border of nares), nares-eye distance (NED, to posterior border of nares to anterior edge of eye), eye-snout distance (ESD, from tip of snout to center of eye), eye diameter (ED, in widest section of the eye), interorbital distance (IOD, between the upper margins of eyes), internarial distance (IND, between the upper margins of nares), length of humerus (LH, from insertion of humerus to elbow), length of forearm (LF, from tip of elbow to wrist), length of thigh (LT, from insertion of femur to knee), length of tibia (LTB, from knee to ankle), width of mental scale (WM, between lateral corners), length of mental scale (LM, between tip of the scale and posterior border with postmentals), width of rostral scale (WR, between lateral corners), and length of rostral scale (LR, between anterior tip of the snout and medial contact with nasals).

Scale counts and terminology follow Rodrigues (1986), and Cassimiro & Rodrigues (2009), and were counted as follows: number of rostrals (R), number of postrostrals (PR), number of postnasals (PN), number of supralabials (SL), number of infralabials (IL), number of mentals (M), number of postmentals (PM), scales that surround the postmentals (SSP), number of ventrals in a longitudinal row (VLR, along a midventral line, from anterior margin of forelimbs to anterior margin of hind limbs), number of dorsal tubercles in a longitudinal row (DT, along a mid-dorsal line, from anterior margin of forelimbs to tail), number of lamellae under the fourth finger (L4F), number of lamellae under the fourth toe (L4T), number of postcloacal tubercles at the sides of the vent (TP), and number of postcloacal pores (CP).

Sex was identified by direct inspection of gonads (when dissected), by the presence of eggs (females) or hemipenis (males, when everted) or by a small lateral insertion at the base of the tail when not everted (presence of the hemipenis or the hemipenial retractor muscle).

To identify sexual dimorphism in SVL, univariate analysis of variance (ANOVA) was performed, and for variation between sexes in the other morphometric characters we used multivariate analysis of variance (MANOVA). The interspecific variation was summarized with Principal Component Analysis (PCA) and Discriminant Function Analysis (DFA) for meristic and morphometric characters separately. In addition, these analyses were performed

for the complete dataset (including all analyzed species) and for a dataset containing only the representatives of *P. pollicaris* complex. All analyses were performed in the R Studio software.

For color descriptions, we used the terminology proposed by Köhler (2012) with their corresponding color codes. For *P. heuteri, P. maranjonensis* and *P. przewalskii* morphological data for comparisons were obtained from literature and/or photographs (Koslowsky 1895; Koch *et al.* 2006; Cacciali *et al.* 2018).

Results

Phylogenetic inference and genetic distance analyses. The dataset included three new 16S rRNA sequences generated in this study (486 pb) and 45 obtained from GenBank. The best evolutionary model for the dataset was GTR + I + G. The Bayesian analysis recovered monophyly for the *P. pollicaris* complex (posterior probability PP = 0.99; Fig. 2). The two individuals from municipality of Mucugê, Bahia state (*Phyllopezus* sp.1), present identical haplotypes and were recovered as the sister clade of individuals from Alagoas state (*Phyllopezus* sp.2), with strong support (PP = 1.0). The three individuals of *Phyllopezus* sp.2 from three different localities in Alagoas state (geographic distance between collecting sites from 33 to 76 km) also present identical haplotypes. The genetic divergence between *Phyllopezus* sp.1 and *Phyllopezus* sp.2 (GD *Phyllopezus* sp.1 × *Phyllopezus* sp.2 = K2P 0.093, p-D 0.087) was similar to that found among other recognized species of the genus (*e.g.*, GD *P. heuteri* × *P. przewalskii* = K2P 0.096, p-D 0.089; see Table 1).

This clade (*Phyllopezus* sp.1 + *Phyllopezus* sp.2, hereafter called as "Group 1" due to the sharing of morphological characteristics, see section Morphological approach) was recovered as sister of the remaining lineages belonging to the *P. pollicaris* complex. The Group 1 corresponds to the sister lineage (PP = 0.99) of the clade composed by *P. heuteri, P. przewalskii* and *P. pollicaris* Clades IV, VI–VIII (hereafter treated as "Group 2"; PP = 0.98). High intraspecific genetic divergences in two methods were observed in *P. pollicaris* clades IV and VII (GD = 0.047 and 0.061, respectively).

Species delimitation analyses. The ABGD analysis indicated the most likely transition point between inter and intraspecific genetic distances around 3–7% (Fig. 3B). The Local Minima function identified a first depression in the distance density curve at 5.73% (N = 1176, Bandwidth = 0.00975). The ABGD analyses did not show great variation between the numbers of delimited genetic clusters and varied from 15 clusters in relative widths of the range less than 1.0 to 16 clusters in relative widths of the range between 1.0 and 1.5 (Fig. 3). The analysis of bPTP and bGMYC recovered 20 genetic clusters, although in bPTP the subdivisions in the clades of *P. przewalskii* and *P. pollicaris* Clade VIII showed low support (less than 95%). Although the cut-off point of 50% was used for the probability of recognition of genetic clusters in bGMYC analysis, it was observed that even adopting a less conservative cut-off point of 90%, only one more genetic cluster was identified. In all analyses *Phyllopezus* sp.1 and *Phyllopezus* sp.2 were recovered as distinct genetic clusters with high statistical support (> 95%).

External morphology. Individuals of *Phyllopezus* sp.1 had significant differences in SVL between sexes (ANOVA: N = 6 ♂, 4 ♀; $F_{1.9}$ = 5.43, P = 0.04). Meanwhile, *Phyllopezus* sp.2 do not show sexual dimorphism in relation to the SVL (ANOVA: N = 9 ♂, 12 ♀; $F_{1.19}$ = 0.15, P = 0.70). However, given the small sample size these observations are not statistically robust. There was also no variation between sexes considering all other morphometric characteristics: *Phyllopezus* sp.1 (MANOVA: $F_{1.19}$ = 2.381, P = 0.105) and *Phyllopezus* sp.2 (MANOVA: $F_{1.8}$ = 0.179, P = 0.906). Morphometric values are available in Appendix III.

When all species were analyzed together (Fig. 4A–D), *P. periosus* and *P. lutzae* were recovered in morphogroups reciprocally segregated in the PCAs and DFAs in all datasets used, with no overlap with the other morphotypes (exceptionally in some *P. periosus* outliers in the PCA for meristic data; Fig. 4A). In relation to the representatives of the *P. pollicaris* complex (Fig. 4C–D), PCAs recovered morphogroups with low overlap, mainly in relation to the representatives of *P. pollicaris* sensu lato.

For analyses performed only with representatives of the *P. pollicaris* complex (Fig. 4E–H), morphogroups with almost no overlap in the morpho-space were recovered. Only in PCA using meristic characters *Phyllopezus* sp.1 and *Phyllopezus* sp.2 showed some degree of overlapping (Fig. 4E).

TABLE 1. Genetic distances between and within species and clades of *Phyllopezus* estimated using Kimura 2-parameters evolutionary model (K2P = bottom right diagonal) and p-distance method (p-D = top left diagonal) with complete deletion of gaps in the 16S rRNA mitochondrial gene fragment. The lowest values of genetic distances between species are highlighted in bold. *Intraspecific genetic distances higher than the cutoff point indicated by the Local Minima analysis. *Phyllopezus pollicaris* Clades follow Werneck *et al.* (2012).

| Species/Clade	1	2	3	4	5	6	7	8	9	10	11	Intraspecific	
												K2P	p-D
1. *P. periosus*	-	0.156	0.169	0.182	0.183	0.181	0.185	0.203	0.187	0.173	0.168	-	-
2. *P. lutzae*	0.177	-	0.135	0.173	0.165	0.176	0.161	0.182	0.154	0.145	0.150	0	0
3. *P. maranjonensis*	0.193	0.150	-	0.181	0.164	0.157	0.170	0.192	0.167	0.156	0.171	0.002	0.002
4. *P. heuteri*	0.211	0.199	0.208	-	**0.089**	0.131	0.129	0.155	0.130	0.139	0.127	0.000	0.000
5. *P. przewalskii*	0.213	0.189	0.186	**0.096**	-	0.112	0.106	0.139	0.110	0.126	0.123	0.023	0.022
6. *P. pollicaris* IV	0.209	0.204	0.177	0.147	0.123	-	0.128	0.155	0.123	0.142	0.148	0.061*	0.057
7. *P. pollicaris* VI	0.214	0.183	0.193	0.144	0.115	0.142	-	0.125	0.097	0.154	0.145	0.004	0.004
8. *P. pollicaris* VII	0.240	0.212	0.224	0.178	0.156	0.177	0.139	-	0.094	0.161	0.154	0.050	0.047
9. *P. pollicaris* VIII	0.217	0.174	0.189	0.145	0.120	0.136	0.105	0.102	-	0.145	0.143	0.021	0.021
10. *Phyllopezus* sp.1	0.198	0.162	0.175	0.155	0.140	0.159	0.174	0.185	0.162	-	**0.087**	0	0
11. *Phyllopezus* sp.2	0.190	0.169	0.194	0.141	0.135	0.168	0.162	0.175	0.160	**0.093**	-	0	0
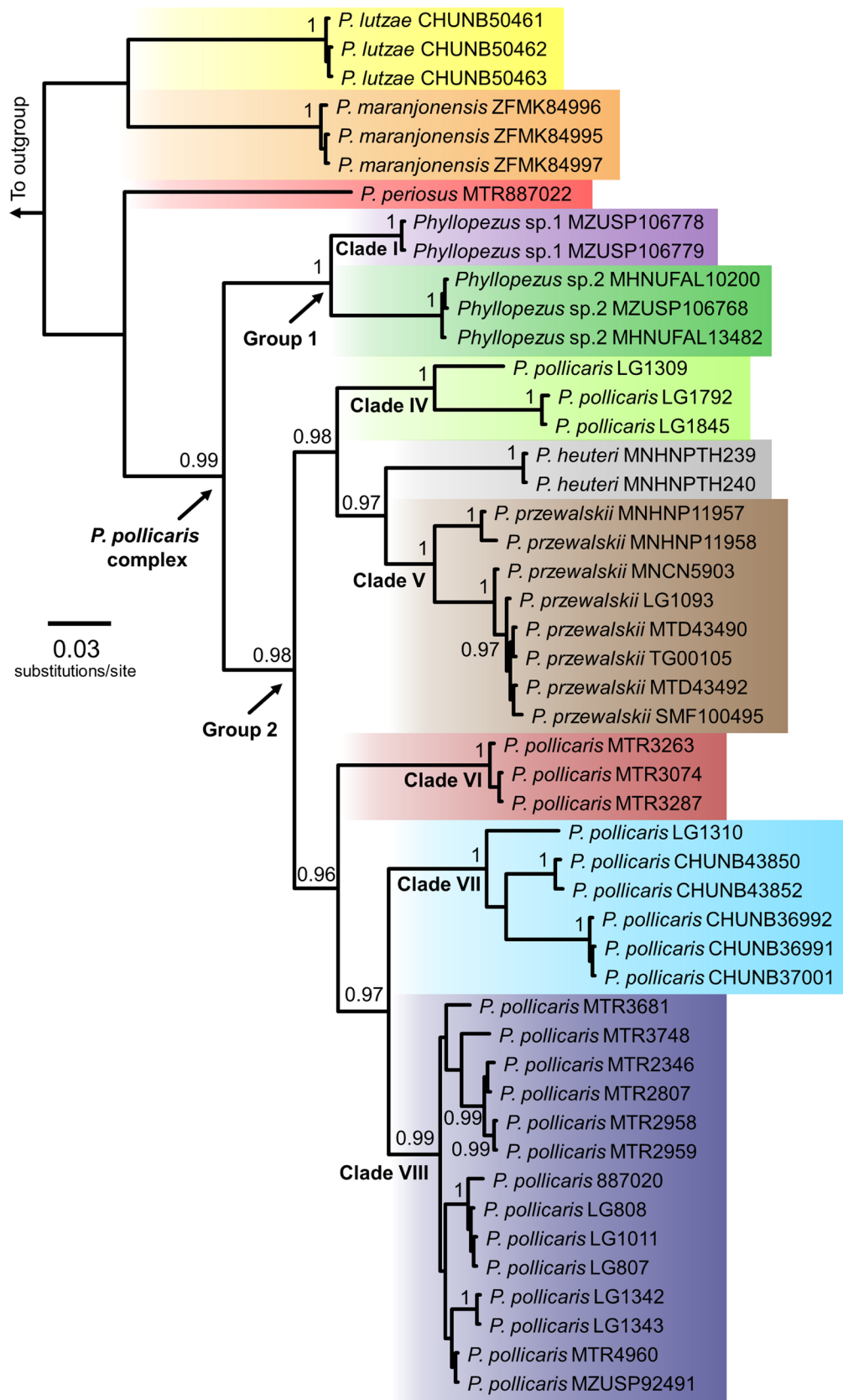
FIGURE 2. Phylogram obtained by the Bayesian Inference of the16S rRNA mitochondrial gene fragment (486 pb) of genus *Phyllopezus*. Posterior probabilities greater than 0.95 are indicated on the nodes. *Phyllopezus pollicaris* Clades I and IV–VIII follow the definitions by Werneck *et al.* (2012). No representatives of the Clades II and III were included due to the lack of 16S rRNA sequences.
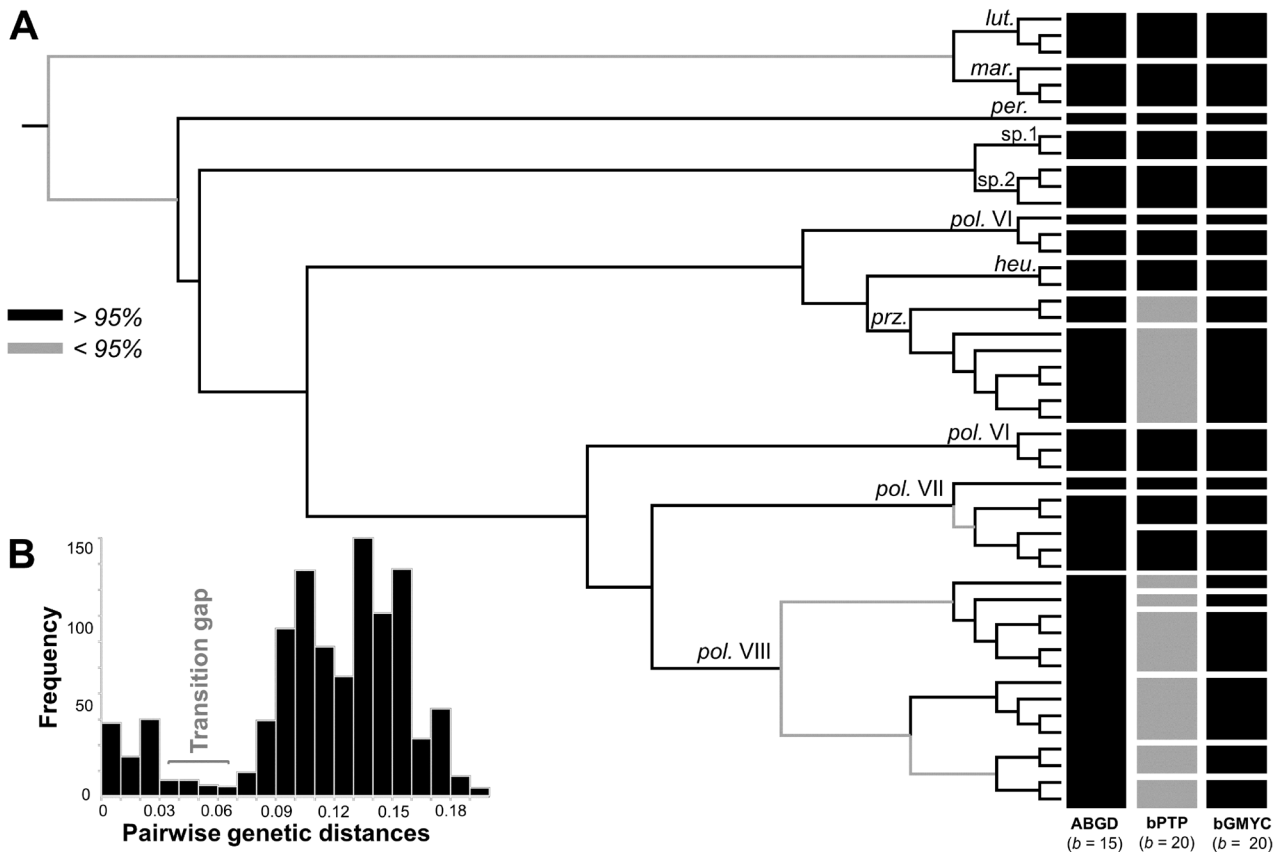
FIGURE 3. (A) Summary results of *Phyllopezus* species delimitations based on 16S rRNA mitochondrial gene fragment using ABGD, bPTP and bGMYC models, respectively. Total genetic breaks found in each model. Abbreviations above nodes: lut. = *P. lutzae*, mar. = *P. maranjonensis*, per. = *P. periosus*, sp.1 = *Phyllopezus* sp.1, sp.2 = *Phyllopezus* sp.2, pol. VI = *P. pollicaris* VI, heu. = *P. heuteri*, prz. = *P. przewalskii*, pol. VI = *P. pollicaris* VI, pol. VII = *P. pollicaris* VII, and pol. VIII = *P. pollicaris* VIII. (B) Pair-to-pair genetic divergence densities indicating the most likely transition gap between intraspecific (left) and interspecific (right) genetic distances of *Phyllopezus* sequences using 347 bp of 16 SrRNA mitochondrial gene fragment. *Phyllopezus pollicaris* Clades numbering follow Werneck *et al.* (2012).

Taxonomic implications. Two main clades are recovered in the *Phyllopezus pollicaris* complex (Group 1 and 2) showing high genetic divergence between them (GD = K2P 0.159, p-D 0.142), similar divergence found between more external specific lineages of the genus (*e.g.*, *P. periosus*, *P. lutzae*, *P maranjonensis*; GD = 0.165–0.195). Morphologically, the lineages belonging to Group 1 can be distinguished from those belonging to Group 2 (in parentheses) by the presence of postmental scales hexagonal-shaped, twice as long as wide (heptagonal-shaped with similar width and length); larger dorsal tubercles, corresponding to about six granules, elongated and generally slightly keeled (smaller dorsal tubercles, corresponding to about four granules, subcircular or elliptical); first rows of reduced scales that surround the enlarged scales of the postmental region do not extend beyond the posterior margin of the third infralabial (always extending beyond the posterior margin of the third infralabial); and their larger size: SVL 88.5 ± 7.25 / 74.4–100.2 (SVL 71.7 ± 5.3 / 59.4–87.1; ANOVA: $F_{1,117}$ = 1.833, P = 0.031). For more details on the variations see the "Comparison with Congeners" section.

Based on the external morphology and genetic data, the two lineages belonging to Group 1 of the *Phyllopezus pollicaris* complex are described herein as new species.

Systematics

***Phyllopezus diamantino* sp. nov.**
(Figs. 5, 6, 9G, 10A)
[http://zoobank.org/urn:lsid:zoobank.org:act:2C6721F5-5F66-4F74-892D-F708B153995D]
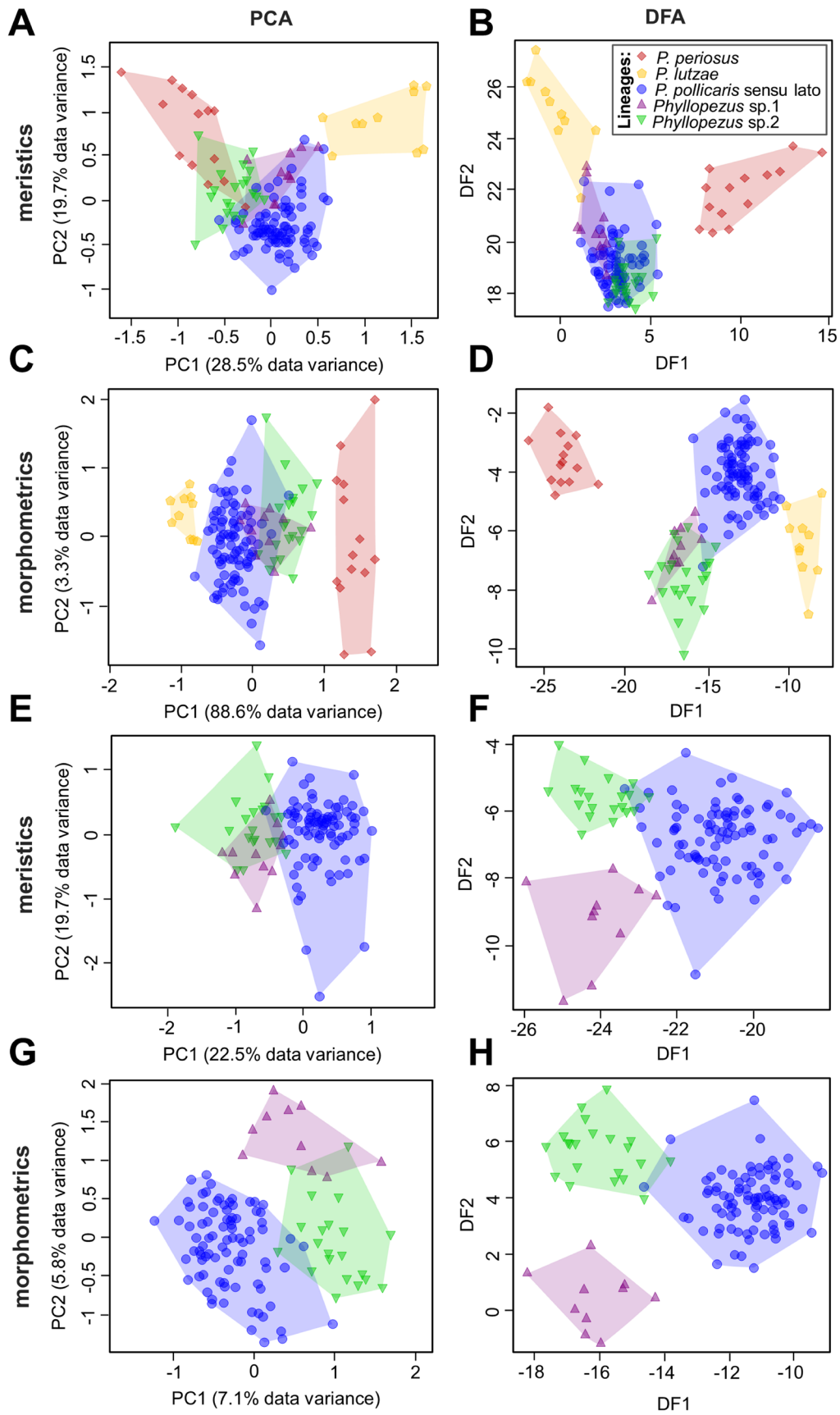
FIGURE 4. Principal Component Analysis (PCA; left) and Discriminant Function Analyzes (DFA; right) based on 13 meristic and 20 morphometric characteristics independently for (A–D) all lineages of *Phyllopezus* and (E–H) only the lineages of *P. pollicaris* complex occurring in northeastern Brazil.

Phyllopezus pollicaris: Cassimiro & Rodrigues (2009); Freitas *et al.* (2012)
Phyllopezus pollicaris Clade A: Gamble *et al.* (2012)
Phyllopezus pollicaris Clade I: Werneck *et al.* (2012); Cacciali *et al.* (2018)
Phyllopezus sp.1 (aff. *pollicaris*): Dubeux *et al.* (*present study*)

Holotype. MZUSP 106770 (adult female) from Serra do Sincorá, Chapada Diamantina [12°59'34"S, 41°20'29"W; 935 m above sea level (a.s.l.)], municipality of Mucugê (Fig. 1C), Bahia state, Brazil, collected on 15 March 2005 by J. Cassimiro and F.S.F. Leite, field number JC 1234.

Paratypes. MZUSP 106771 (adult female; 13°00'03"S, 41°21'58"W; 999 m a.s.l.), MZUSP 106772 (adult female; 13°01'26"S, 41°21'53"W; 980 m a.s.l.), MZUSP 106773 (adult female; 13°00'19"S, 41°21'47"W; 1010 m a.s.l.), MZUSP 106778 and MZUSP 106774 (adult male and adult female, respectively; 13°00'16"S, 41°21' 47"W; 1007 m a.s.l.), MZUSP 106775 (adult female; no coordinates), MZUSP 106776 (adult male; 13°01'08"S, 41°21'56 W; 1018 m a.s.l.), MZUSP 106778 (adult male; 13°00'18"S, 41°21'47"W; 1000 m a.s.l.), MZUSP 106779 (adult male; 13°01'02"S, 41°20'39"W; 945 m a.s.l.), MZUSP 106781 and MZUSP 106780 (juvenile unsexed and adult male, respectively; 13°00'05"S, 41°21'57"W; 983 m a.s.l.), MZUSP 106782 (juvenile unsexed; 13°00'03"S, 41°21'58"W; 999 m a.s.l.). All paratypes are topotypes and were collected between 3–17 March 2005, by J. Cassimiro, F.S.F. Leite and L.E. Lopes.

Etymology. The specific epithet "*diamantino*" is a latinized adjective referring to its type-locality, *Parque Nacional da Chapada Diamantina*, the northern segment of the *Cadeia do Espinhaço* in the state of Bahia, Brazil.

Diagnosis. *Phyllopezus diamantino* **sp. nov.** is characterized by the following combination of character states: (1) Mental scales sub-triangular, with similar length and width and posterior margin not exceeding the second infralabial; (2) postmental scales increased, hexagonal, twice as long as wide, with broad contact each other and previously separated by about 1/3 of its length by the mental scale; (3) up to two scales in contact with the ventral margin of first infralabial; (4) presence of enlarged scales surrounding and separating postmental scales from the granules of the gular region; (5) six to seven infralabial scales; (6) granular scales in the distal region of mandible, juxtaposed, occasionally presenting tubercles of different sizes; (7) dorsal tubercles enlarged, corresponding to about six granular scales, elongated and keeled; (8) developed pollex; (9) cycloid or triangular scales around the auditory meatus, little bristly; (10) homogeneous scales of the same size in the region of the labial commissure; (11) many tubercles in the angular region between the upper and lower edges of the opening of the auditory meatus and eyes; (12) postcloacal pores always present in males and females; and (13) large sized, SVL 76.41–96.25 mm in males, and 72.38–82.36 mm in females. See "Comparison with Congeners" section for additional diagnosis with other genus species.

Description of holotype. Adult female, SVL 96.25, fully regenerated tail, DBL 37.97, TBW 10.12, HL 27.75, HW 19.17, HD 8.73, SL 11.01, NSD 2.42, ESD 8.82, ED 6.94, IOD 8.87, IND 3.27, LH 21.04, LF 13.13, LT 22.02, LTB 15.41, WM 4.41, LM 4.28, WR 4.05, LR 2.16, R 1, PR 3, SN 2, SL 7, IL 7, M 1, PM 2, SSP 7, VLR 59, DT 45, L4F 10, L4T 14, TP 3, and CP 1. Head large (SVL/HL = 3.43), distinct from neck. Mental large (HW/WM = 4.3 and HL/LM = 6.4), sub-triangular, slightly wide than longer (WM/LM = 1.03), bordered by the 1st infralabial and in broad contact with two postmentals. A pair of postmentals, large, hexagonal-shaped, juxtaposed, longer than wide, separated for mental by one third of their length, flanked by seven large scales with differentiated sizes, which are replaced by granules juxtaposed that extend to the level of the labial commissure and are gradually replaced by similar small scales, smooth and imbricate, similar to ventral scales. First five infralabials rhomboid; the first largest, in broad contact with the postmental pair and a group of seven large, smooth, variable-shaped scales that isolate the postmentals from the granules of the gular region. These are succeeded by small scales that undergo abrupt reduction in size until become granules in the beginning of the gular region. First infralabial smaller than 2nd, and from the 2nd on decreasing in size towards the labial commissure; the commissure area with granules. First to 4th infralabial scales rhomboid. From the 2nd infralabial on, there is a group of small, elongated scales that border the infralabial row to near of the labial commissure, which also isolates them from the granules of the gular region. Ventral scales smooth and imbricate, cycloid, arranged in longitudinal rows. Large rostral (HW/WR = 4.7 and HL/LR = 12.8), wider than long (WR/LR = 1.8), triangular, visible in dorsal view, with a fissure extending from the region in contact with the nasal to half of the rostral, and a perforation in the upper left side. A pair of postrostrals protruding, separated by two tiny scales and in contact with the one of postnasals. Large supralabials, longer than wide, decreasing in size to the end of the labial commissure. First supralabial in broad contact with the rostral and one of the postnasals, involving part of the nostril. Posterior snout region and interorbital region concave. Dorsal and lateral surfaces of the head covered

with granular juxtaposed scales, with scattered tubercles on the upper surface starting at the level of interorbital region. Granules in the snout larger than those of the occipital region. Eighteen small granules between the postnasals and anterior ocular margin. The granules surrounding the ocular region are tiny and more spaced than those of the snout and the dorsum. Postnasals swelling, elongated and bordering 1/4 of the nostril. The border of the auditory meatus is surrounded by small scales and granules. In the auditory meatus, the scales are small and smooth. Dorsal region of the body covered by granular scales and larger tubercles almost equidistant, conical and anteroposteriorly elongated, arranged in 10 to 14 irregular lines, reaching the level of the posterior region of hindlimbs, just before tail insertion. Postcloacal tubercles present, three on each side, easily perceived. Postcloacal pores present, one on each side. Regenerated tail, presenting smaller overlapping cycloid scales in the dorsal region and increasing in size in the lateral region. A row of smooth, elongated medial scales in the ventral region of the tail, two or three times wider than long, covering to half of the ventral region of tail. Dorsal surface of the forelimbs and hindlimbs different of the dorsum of the body, with medium scales smooth and imbricate, tubercles absent. Palmar and plantar regions with small granules, replaced in the forearms by smooth, cycloid, and imbricated scales. Infradigital lamellae on the 4th finger of the forelimbs and hindlimbs wider than long, wider than high, almost straight; two distal lamellae in open V-shaped. Claws bordered by smooth and imbricate scales, composed of five scales in the ventral region, five dorsal scales. Side of claws with two rows of scales with five scales each. Presence of sheath with three scales.

Coloration in life (Fig. 6 and 10A)**.** Based on a not collected topotype: Body with background color Olive Horn (16). The dorsum has irregular bands on sides beginning in the postnasal region and extending towards the base of the tail; these bands show irregular stains in the Sepia (229) surrounded by Pale Cinnamon (55) tones. Small irregular spots with Brownish Olive (276) tones distributed along the dorsum of the body and limbs. A lateral band in the head beginning in the labial commissure (rather than dashes), Sepia (229) and Pale Cinnamon (55) colors, that extends until the hindlimbs. Limbs in Sepia (229) and Sulphur Yellow (91) pattern with irregular spots in Brick Red (36) up to the claws. Head Olive Horn (16). Irregular Brownish Olive (276) spots between the eyes and the auditory meatus. Tail with well-defined transverse bands alternating between Olive Horn (16) and Sepia (229) with Brownish Olive (276) spots. In the beginning of the tail, there is a Brownish Olive (276) triangular-shaped spot. The regenerated segment of the tail is an Olive Horn (16) that do not form a distinguishable pattern. Ventral region Sulphur Yellow (91), without spot pattern. Infradigital lamellae Pale Mauve (204).

Coloration in preservative (Fig. 5)**.** The color pattern of holotype differs significantly from the coloration of the topotype in life described above. The dorsal pattern is almost homogeneous with little contrast between the irregular bands and background coloring (although these are visible when looking more closely). The background color is Dark Drab (45) and the bars are Brunt Umber (48). The tail region (regenerated) has a lighter color in Drab (19) and the ventral region becomes Pale Horn Color (11) slightly darker.

Intraspecific variation. All diagnostic characteristics for the new species are seen in all specimens analyzed. The MZUSP 106772 specimen does not present postcloacal tubercles and the MZUSP 106776 lacks a postrostral scale. Morphometric variation and the scale count range among specimens are provided in Appendix III.

Distribution, habitat, and natural history. The new species is currently known only from the mountains of Serra do Sincorá, in the Chapada Diamantina, an area situated in the northern segment of Espinhaço mountain range. A mosaic of vegetation types, of which "campos rupestres", or rupestrian grasslands, a dominant open-rock pioneer vegetation with rock-dwelling plants, are most common, characterizes the area. Notwithstanding, there are varieties of other environments in the region, like gallery forests, "Cerrado" (savanna-like), montane forests and semi-deciduous to deciduous forests (Giulietti & Pirani 1988).

Phyllopezus diamantino **sp. nov.** is nocturnal and specimens were found on rocky outcrops and in tree and shrub trunks. Active animals were found only at night on the surface of rocks or trees or in rock crevices, and during the day only one inactive specimen was found under a rock.

Gymnodactylus vanzolinii and *Hemidactylus brasilianus* were observed syntopically with *P. diamantino* **sp. nov.** on the rocks or in rock crevices, even though the new species was also found in other microhabitats as tree and shrub trunks. Other lizards observed and recorded at Mucugê area were: *Hemidactylus mabouia* (Gekkonidae), *Acratosaura mentalis*, *Acratosaura spinosa*, *Heterodactylus septentrionalis*, *Micrablepharus maximiliani*, *Psilops mucugensis* (Gymnophthalmidae), *Enyalius erythroceneus* (Leiosauridae), *Polychrus acutirostris* (Polychrotidae), *Brasiliscincus heathi* (Scincidae), *Ameiva ameiva*, *Ameivula* cf. *ocellifera*, *Tupinambis merianae* (Teiidae), *Eurolophosaurus* sp., *Tropidurus hispidus*, *T. mucujensis*, and *T. semitaeniatus* (Tropiduridae) (Freitas & Silva 2007; Cassimiro & Rodrigues 2009).
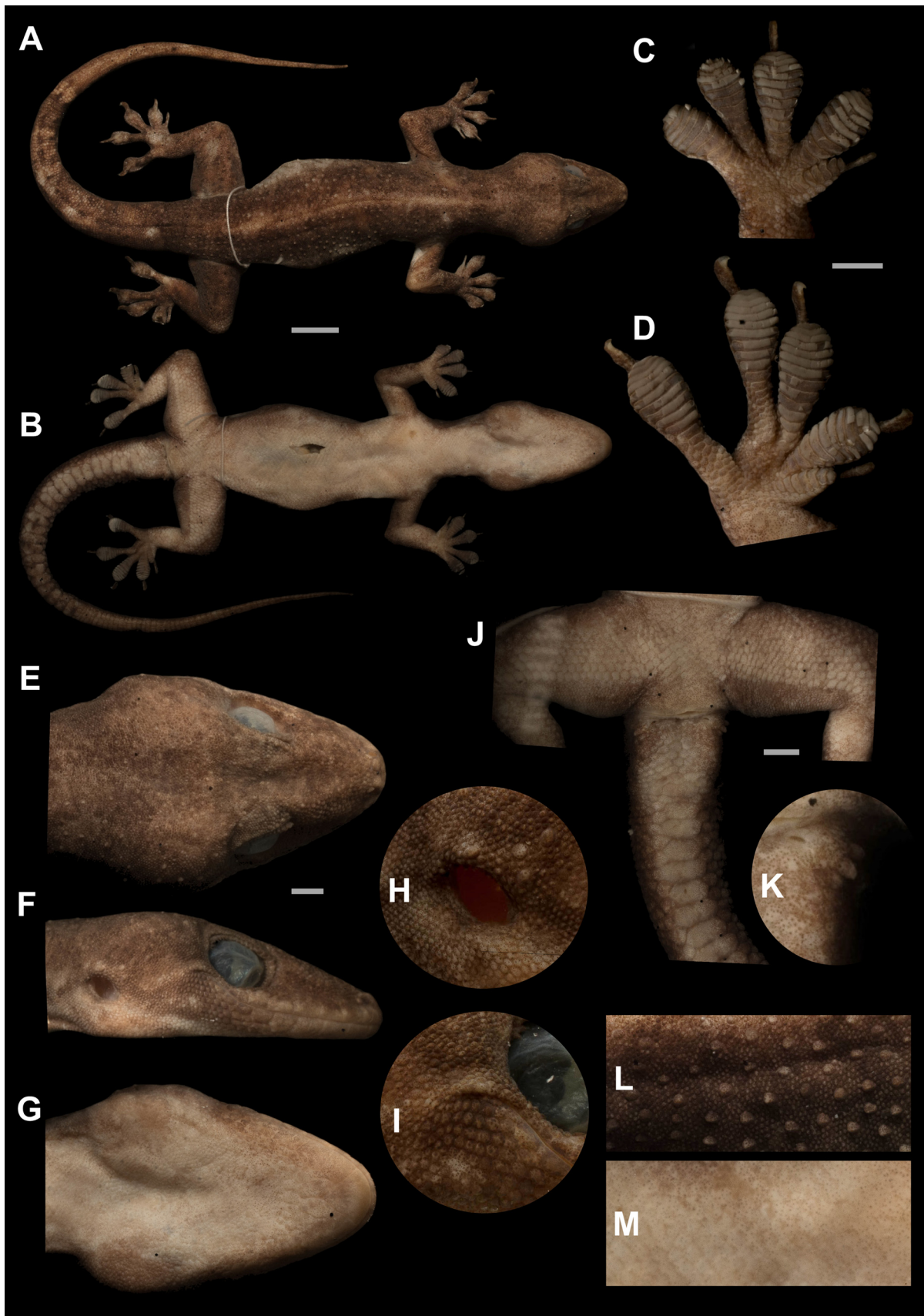
FIGURE 5. Holotype of *Phyllopezus diamantino* **sp. nov.** (MZUSP 106770, adult female). A and B = dorsal and ventral views of body; C = palm of hand; D = sole of the foot; E–G = dorsal, lateral and ventral views of head; H = auditory meatus; I = labial commissure; J = cloacal region; K = tubercles and postcloacal pores on the left side of the body; L = tubercles and dorsal scales; M = ventral scales. Scale bar = A and B (10mm), C–G and J (3mm).

FIGURE 6. Color in life of topotype (unvouchered specimen) of *Phyllopezus diamantino* **sp. nov.**

Phyllopezus selmae **sp. nov.**
(Figs. 7, 8, 9H, 10B)
[http://zoobank.org/urn:lsid:zoobank.org:act:226D6FA9-804A-4A9B-9303-160F876A7F41]

Hemidactylus mabouia: Roberto *et al.* (2015: part, p. 715, fig. 7)
Phyllopezus sp.: Gonçalves & Palmeira (2016)
Phyllopezus sp.2 (aff. *pollicaris*): Dubeux *et al.* (*present study*)

Holotype. MHNUFAL 13481 (adult female) from Cariri da Prensa Farm (9°41'41"S, 36°12'16"W; 83 m a.s.l.), municipality of Boca da Mata (Fig. 1B), Alagoas state, Brazil, collected on 15 January 2014 by U. Gonçalves and C. Palmeira, field number UGS 702.

    Paratypes. Adult female (MHNUFAL 13482) collected on 3 January 2017, from the same locality of holotype (topotypes); adult females (MHNUFAL 12169, CHUFPE-R 1002, 1003) and adult males (MHNUFAL 12168, 12172, CHUFPE-R 1004) collected on 9 July 2015, adult females (MZUSP 106766, 106767) and adult males (CHUFPE-R 1005, MZUSP 106768) collected on 20 January 2015, and adult males (MHNUFAL 12396, 12397, 12399, 12400, MZUSP 106769) collected on 16 November 2015, from municipality of Limoeiro de Anadia (Fig. 1B), Alagoas state, Brazil (9°47'05"S, 36°28'04"W; 117 m a.s.l.); adult female (MHNUFAL 12449) and adult male (MHNUFAL 12128) collected on 7 July 2015, from municipality of Coruripe (Fig. 1B), Alagoas state, Brazil (10°03'17"S, 36°16'32"W; 68 m a.s.l.); adult females (MHNUFAL 10200) collected on 23 January 2015, from municipality of Igaci (Fig. 1B), Alagoas state, Brazil (9°32'00"S, 36°36'43"W; 269 m a.s.l.), all paratypes above were collected by U. Gonçalves and C.N.S. Palmeira; adult male (MHNUFAL 12401) collected on 13 June 1999 by Selma Torquato, adult male (MHNUFAL 16198) and juvenile unsexed (MHNUFAL 16199) collected on 21 April 2019 by M.J.M. Dubeux, from municipality of Quebrangulo (Fig. 1B), Alagoas state, Brazil (9°15'22"S, 36°25'43"W; 780 m a.s.l.).

Etymology. The name of species is in honor of Selma Torquato, curator of Coleção Herpetológica do Museu de História Natural da Universidade Federal de Alagoas who has generously provided many opportunities for herpetologists to study the amphibian and reptile specimens under her care.

Diagnosis. *Phyllopezus selmae* **sp. nov.** is characterized by the following combination of characters: (1) Mental scales in bell shaped, with concave margins and a slight central constriction, similar length and width and posterior margin not exceeding the second infralabial; (2) postmental scales enlarged, hexagonal, twice as long as wide, with broad contact each other and previously separated by about 1/5 of its length by the mental scale; (3) up to two scales in contact with the ventral margin of first infralabial; (4) enlarged scales surrounding and separating postmental scales from granules of the gular region; (5) six to seven infralabial scales; (6) cycloid and imbricated scales of similar size in distal region of mandible; (7) enlarged dorsal tubercles, corresponding to about six granular scales, elongated and slightly keeled; (8) developed pollex; (9) cycloid or triangular scales around the auditory meatus, appears somewhat bristly; (10) homogeneous scales of the same size in the region of the labial commissure; (11) up to two tubercles or tubercles absents in the angular region between the upper and lower edges of the opening of the auditory meatus and eyes; (12) postcloacal pores not always present; and (13) large sized, SVL 89.2–100.24 mm in males, and 83.5–99.47 mm in females. See Comparison with congeners section for more additional diagnosis with other species.

Description of holotype. Adult female, SVL 99.47 mm, fully regenerated tail, DBL 42.82 mm, TBW 12.31 mm, HL 27.02 mm, HW 19.53 mm, HD 9.2 mm, SL 11.08 mm, NSD 2.73 mm, ESD 8.29 mm, ED 6.09 mm, IOD 8.42 mm, IND 3.79 mm, LH 20.11 mm, LF 12.23 mm, LT 20.88 mm, LTB 15.3 mm, WM 4.64 mm, LM 4.98 mm, WR 4.54 mm, LR 2.3 mm, R 1, PR 2, SN 2, SL 8, IL 7, M 1, PM 2, SSP 7, VLR 51, DT 43, L4F 14, L4T 13, TP 2, and CP 0. Head large (SVL/HL = 3.68), distinct from neck. Mental large (HW/WM = 4.2 and HL/LM = 5.4), bell-shaped, slightly longer than wide (WM/LM = 0.93), narrower posteriorly and with a slight strangulation in its half, bordered by the 1st infralabial and in broad contact with two postmentals that separated it from others infralabial and gular scales. A pair of postmentals, large, hexagonal, juxtaposed, longer than wide, and flanked by seven large scales with differentiated sizes, which are replaced by small scales, smooth and imbricate, similar to ventral ones. First, 2nd and 3rd infralabials rhomboid; 1st the largest, in contact with the postmental pair, and a group of five large, smooth and variable in shape scales that isolate the pair of postmentals from scales in the gular region. The infralabials decrease in size towards the labial commissure; commissure area with granules. From the 2nd infralabial, there is a group of small, elongated scales that border the infralabial row near of the labial commissure, which also isolates them from the granules of the gular region. Ventral scales smooth and imbricate, cycloid, arranged in longitudinal rows. Large rostral (HW/WR = 4.3 and HL/LR = 11.74), wide than longer (WR/LR = 1.97), triangular-shaped, with a median depression at the top where there is a fissure extending from the region in contact with the nasal to half of the rostral. Large supralabials, longer than wide, decreasing in size to the end of the labial commissure. First supralabial in broad contact with the rostral and one of the postnasals, involving part of the nostril. Dorsal and lateral surfaces of the head covered with granular juxtaposed scales, with scattered tubercles on the upper surface starting at the level of interorbital region. Granules in the snout four to five times larger than those of the occipital region. Fifteen small granules between the postnasals and anterior ocular margin. The granules surrounding the ocular region are tiny and more spaced than those of the snout or the dorsum. The supranasal region involves half of the nasal fossa. Postnasals swollen, elongated and bordering 1/3 of anterior portion of the nostril. The border of the auditory meatus is surrounded by small granules. In the auditory meatus, the scales are erect and acicular, triangular, smooth and imbricate. Dorsal region of body covered by granular scales and almost equidistant larger tubercles, conic and elongated anteroposteriorly, arranged in 11 to 14 irregular lines, reaching the level of the posterior region of the hindlimbs (before the tail insertion). Postcloacal tubercles present, a pair on each side, very conspicuous. Postcloacal pores absent. Regenerated tail, presenting smaller overlapping cycloid scales in the dorsal region and increasing in size in the lateral region. A row of smooth, elongated medial scales in the ventral region of tail, three or four times wider than long, covering almost the entire ventral region. Dorsal surface of the forelimbs and hindlimbs, with medium sized scales, smooth and imbricate; tubercles absent. The small granules in the palmar and plantar regions are replaced by smooth, cycloid, and imbricated scales in the forearms. Infradigital lamellae on the fourth finger and fourth toe wider than long, wider than high, slightly arched and becoming straighter in the distal portions. Claws bordered by smooth and imbricate scales, composed of five scales in the ventral region, five dorsal scales. Side of the claws with two rows of scales with five scales each. Presence of sheath with three scales.
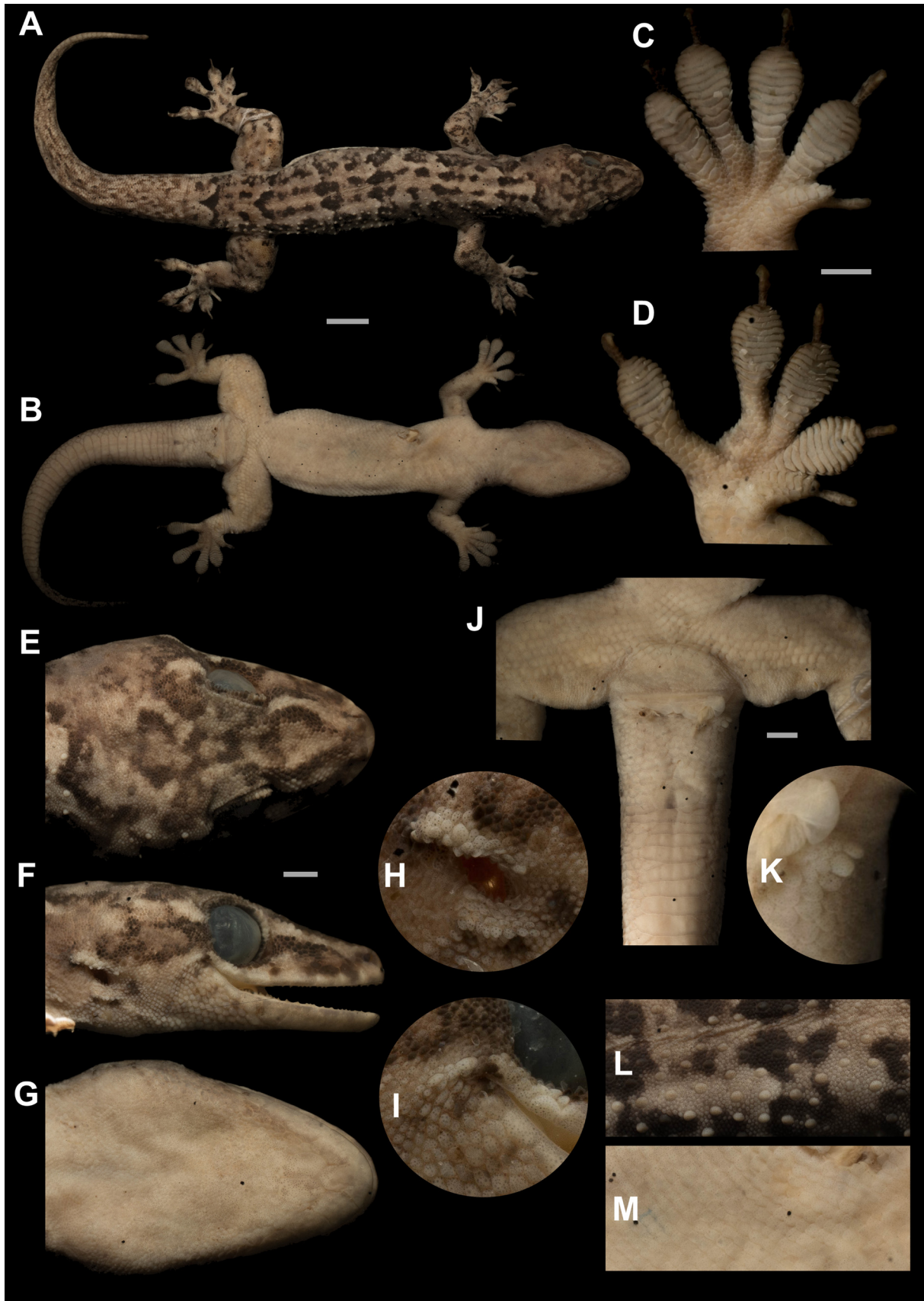
FIGURE 7. Holotype of *Phyllopezus selmae* **sp. nov.** (MHNUFAL 13481, adult female). A and B = Dorsal and ventral views of body; C = palm of hand; D = sole of the foot; E–G = dorsal, lateral and ventral views of head; H = auditory meatus; I = labial commissure; J = cloacal region; K = tubercles on the left side of the body; L = tubercles and dorsal scales; M = ventral scales. Scale bar = A and B (10mm), C–G and J (3mm).

Coloration in life (Fig. 8)**.** Based on holotype: Body with background color Raw Umber (22). The dorsum with semicontinuous longitudinal bands, on sides beginning in the postnasal region and extending towards the base of the tail; band near the dorsal midline begins in the nuchal region; these bands show irregular dashes in the Dusky Brown (285) surrounded by Sayal Brown (41) tones. Small irregular spots in the Pale Horn Color (11) tones distributed along the dorsum of the body and limbs. A lateral band in the head beginning in the labial commissure (rather than dashes), Dusky Brown (285) color, that extends until the hindlimbs. Limbs in Raw Umber (22) pattern with irregular spots in Dusky Brown (285) and Sayal Brown (41) up to the claws. Head Raw Umber (22), superimposed by irregular spots Dusky Brown (285). Snout with a triangular-shaped Army Brown (46) spot, surrounded by Dusky Brown (285). Irregular Dusky Brown (285) spots between the eyes and the auditory meatus. Tail with well-defined transverse bands alternating between Raw Umber (22) and Sayal Brown (41) with Dusky Brown (285) spots. In the beginning of the tail, there is a Dusky Brown (285) triangular-shaped spot. The regenerated segment of the tail is a Raw Umber (22) color that is overlaid by Sayal Brown (41) spots that do not form a distinguishable pattern. Ventral region Pale Horn Color (11), without spot pattern. Infradigital lamellae Pale Mauve (204).

Coloration in preservative (Fig. 7)**.** In general, the coloration in preservative does not differ substantially from life coloration. The background color becomes similar to Beige (254), tending to a more grayish tone. The longitudinal bands retain their color; however, they lose the Sayal Brown color (41) that surrounds them in life, becoming more prominent in relation to the background. On the dorsal surface of the limbs and in the regenerated portion of the tail, the Sayal Brown color (41) becomes Fawn Color (258) and the ventral region becomes Pale Horn Color (11) slightly darker.

Intraspecific variation. All diagnostic characters used for describing the new taxon are present in all specimens analyzed. However, different dorsal background coloration in life were observed, depending on the time and type of the substrate of capture, ranging from Raw Umber (22) to Drab (19). Ontogenetic variations of color were also observed; a juvenile (MHNUFAL 16199; Fig. 8C) presents a more demarcated dark longitudinal bands and Pale Buff (1) lighter color background. Morphometric and meristic variation are provided in Appendix III.
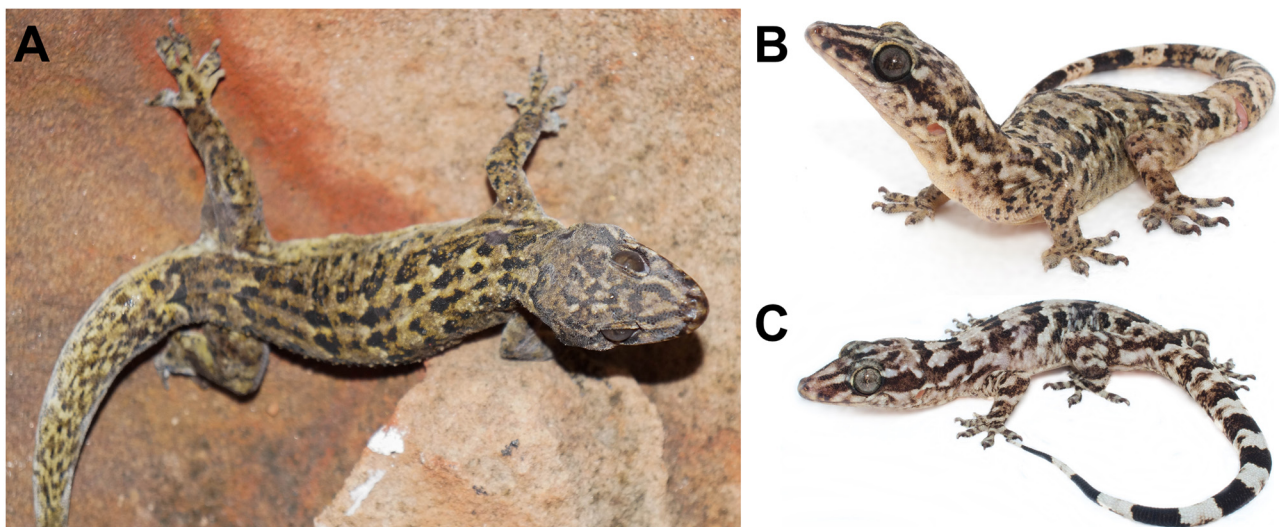

FIGURE 8. Coloration in life of *Phyllopezus selmae* **sp. nov.** (A) Holotype [MHNUFAL 13481], (B and C) paratypes [MHNUFAL 16198 and MHNUFAL 16199, respectively], (C) variation of juvenile coloration.

Distribution, habitat, and natural history. *Phyllopezus selmae* **sp. nov.** is a nocturnal species found in rocky outcrops and trees, in heights up to 10 m. In the daytime, specimens were found sheltering either under tree bark, clumps of epiphytes or bromeliad roots. Animals were mainly observed active in the early evening when foraging in forested sites near rivers with rocky bed. The species was also found sharing bromeliads with *P. lutzae*. When specimens were captured, they twisted their body by turning quickly to the side, and when attempting to bite would produce an agonistic "squeaking" sound (not recorded). The distribution of the species is only known for the state of Alagoas, with altitudes ranging from 68 m in the municipality of Coruripe to 780 m a.s.l. at the top of the rock formation of *Pedra Talhada*, municipality of Quebrangulo (Fig. 1).

DUBEUX *ET AL.*

Comparisons with congeners. *Phyllopezus diamantino* **sp. nov.** and *Phyllopezus selmae* **sp. nov.** are morphologically more similar to each other than to the other representatives in the genus and together are distinguished from the congeners mainly by characters in the gular region (Fig. 9). Both new species (Fig. 9G–H) differ from *P. periosus* (Fig. 9A) by the presence of increased scales separating the postmentals granules in the gular region (absent in *P. periosus*), posterior margin of the mental scale not exceeding the anterior margin of the second infralabial scale (exceeding the anterior margin of the second infralabial in *P. periosus*) and postmental scales in direct contact (separated by the mental scale in *P. periosus*). Both new species differ from *P. lutzae* (Fig. 9B) by presenting a long mental scale, with similar length and width (short mental with a length corresponding to half the width in *P. lutzae*), posterior margin of the posmental scales exceeding half of the second infralabial (not reaching the second infralabial in *P. lutzae*) and up to two scales in contact with the first infralabial (three to four scales in contact with the ventral margin of the first infralabial in *P. lutzae*). Both new species differ from *P. maranjonensis* (Fig. 9C) in having the central pair of postmentals distinctly larger than the scales that surround them and in contact with the first infralabial (almost the same size and separated from the first infralabial by one or two scales in *P. maranjonensis*). Both new species differ from *P. maranjonensis* and *P. heuteri* in having six or seven infralabial scales (7–10 in *P. maranjonensis* and 8–9 in *P. heuteri*). Both new species differ from *P. maranjonensis*, *P. heuteri* (Fig. 9F), *P. pollicaris* sensu stricto (Fig. 9D) and *P. przewalskii* (Fig. 9E) in having postmental scales twice longer than wide (postmentals with similar width and length in *P. maranjonensis*, *P. heuteri*, *P. pollicaris* and *P. przewalskii*).
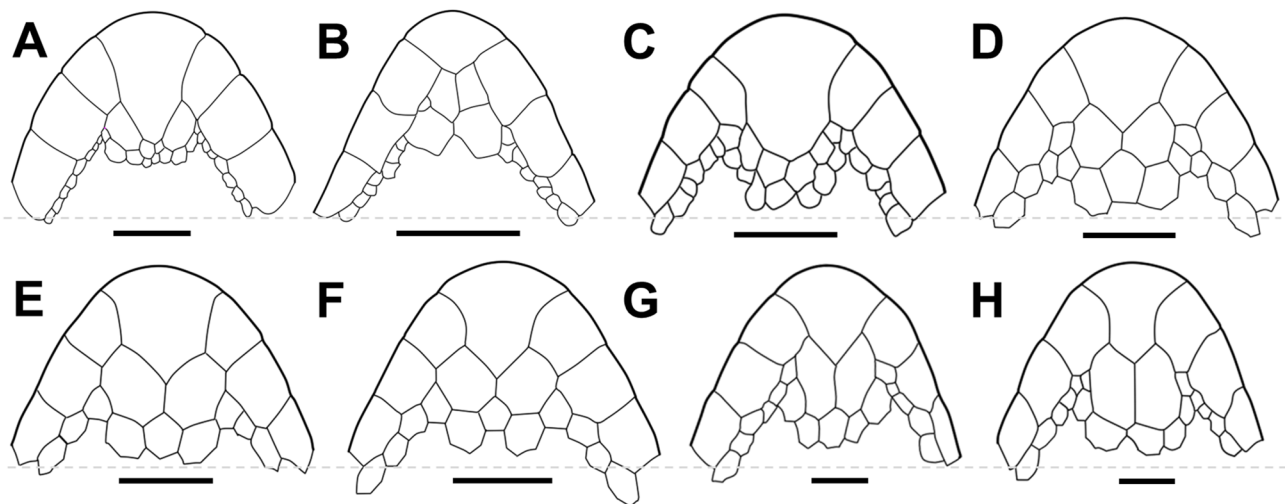

FIGURE 9. Scheme of the arrangement of scales in the gular region of *Phyllopezus* species. (A) *P. periosus* [based on CHUFPB 1936], (B) *P. lutzae* [based on CHUFPB 19518], (C) *P. maranjonensis* [based on ZFMK 84997], (D) *P. pollicaris* stricto sensu [ZSM 165/0/1, paralectotype], (E) *P. przewalskii* [based on SMF 100496], (F) *P. heuteri* [based on SMF 100494], (G) *Phyllopezus diamantino* **sp. nov.** [based on MZUSP 106770] and (H) *Phyllopezus selmae* **sp. nov.** [based on MHNUFAL 13481]. Figures D–F adapted of the photographs provided by Cacciali *et al.* (2018). Horizontal dashed gray line marks the posterior margin of the third infralabial scale. Scale bars = 3mm.

The two new species can also be distinguished from *P. periosus* in having a color pattern in longitudinal or transverse dark irregular dorsal bars (6 to 7 well-defined light-colored transverse bands limited anteriorly and posteriorly by bars dark in *P. periosus*). The two new species can be distinguished from *P. lutzae* in being distinctly larger (72.38–96.25 mm in *Phyllopezus diamantino* **sp. nov.** and 83.50–100.24 mm in *Phyllopezus selmae* **sp. nov.** versus a maximum of 62.77 mm in *P. lutzae*), in having a coloration pattern in irregular longitudinal or transverse dorsal dark bars (homogeneous orange marbled pattern in *P. lutzae*). Both new species can be distinguished from *P. lutzae* and *P. maranjonensis* in having larger dorsal tubercles, corresponding to about six granules (indistinct dorsal tubercles in *P. lutzae* and few slightly enlarged tubercles on the back, rarely forming rows on *P. maranjonensis*). Both new species can be distinguished from *P. lutzae* in having developed pollex (absent or poorly developed in *P. lutzae*). The two new species can be distinguished from *P. maranjonensis* in having a pattern of coloration in irregular longitudinal or transverse dorsal dark colored bars (four regular dark colored cross bars between the neck and vent in *P. maranjonensis*), and six to eight supralabial scales (8–10 in *P. maranjonensis*). Both new species

can be distinguished from *P. heuteri* in having cycloid or triangular scales around the auditory meatus, little bristly (spiny and bristling scales in *P. heuteri*).

FIGURE 10. Coloration in life of dorsal view of the body and dorsolateral view of head of (A) *Phyllopezus diamantino* **sp. nov.** [topotype (unvouchered specimen)] and (B) *Phyllopezus selmae* **sp. nov.** [paratype (MHNUFAL 16198)].

Phyllopezus diamantino **sp. nov.** can be differentiated from *Phyllopezus selmae* **sp. nov.** due to the presence of granular and juxtaposed scales in the distal region of mandible, and may present tubercles of different sizes (cycloid and imbricated scales, of similar size in *Phyllopezus selmae* **sp. nov.**), mental scale triangular with almost straight lateral edges (bell-shaped with concave margins and a slight strangulation in its half in *Phyllopezus selmae* **sp. nov.**; Fig. 9), and anterior portion of the postmental scales separated by almost 1/3 of the length by the mental scale (versus separated by 1/5 in *Phyllopezus selmae* **sp. nov.**; Fig. 9), dorsal coloration pattern in dark transverse bands interrupted by a light cervical band (dark bands arranged in well-defined or transverse longitudinal rows showing interruptions, light cervical band absent or not evident in *Phyllopezus selmae* **sp. nov.**; Figs. 5–8 and 10), four to six tubercles in the angular region between the upper and lower edges of the opening of the auditory meatus and eyes (up to two tubercles or tubercles absents in this region in *Phyllopezus selmae* **sp. nov.**; Figs. 5F and 7F), homogeneous scales of the same size in the region of the labial commissure (increased scales on the upper and lower sides of the labial commissure in *Phyllopezus selmae* **sp. nov.**; Figs. 5I and 7I), and a pair of postcloacal pores is always present (not always present in *Phyllopezus selmae* **sp. nov.**, Figs. 5K and 7K). Morphometric variations and the scale counts range among specimens analyzed are provided in Appendix III.

Discussion

In addition to the cryptic diversity already recognized for the *Phyllopezus pollicaris* complex (Gamble *et al.* 2012; Werneck *et al.* 2012; Cacciali *et al.* 2018), the loss of the lectotype (ZSM 2510/0; Michael Franzen comm. pers. in Cacciali *et al.* 2018) has hampered taxonomic arrangements involving the group. *Phyllopezus pollicaris* was described by Spix (1825) as *Thecadactylus pollicaris* almost 200 years ago, to accommodate a population in the interior of the state of Bahia ("*in sylvis interioris Bahiae campestribus*"), with no further locality data (Spix 1825; Vanzolini 1953).

In Bahia state, a high diversity of lineages belonging to the *P. pollicaris* complex were found, some of them are not closely related (*P. diamantino* **sp. nov.** [previously *P. pollicaris* Clade I] and *P. pollicaris* Clades III, VI and VIII; Werneck *et al.* 2012; Cacciali *et al.* 2018; *present study*). All the diagnostic characters for both of the new species and the comparisons with congeners were based on the photographs of the paralectotypes of *P. pollicaris* [ZSM 165/0/1–2; according to Müller & Brongersma (1933) those specimens were in the original type series], in the

detailed description of these provided by Müller & Brongersma (1933) and Cacciali *et al.* (2018), and in the original description by Spix (1825). We observed that the *P. pollicaris* paralectotypes are morphologically similar to lineages belonging to Group 2 (*P. heuteri* + *P. przewalskii* + *P. pollicaris* Clades IV, VI–VIII). They share characteristics such as number, size, format and disposition of the gular scales and its small size (see "Taxonomic Implications" and "Comparison with Congeners" sections). Although the municipality of Mucugê is located in Bahia, the same Brazilian state where the type-locality of *P. pollicaris* sensu stricto is located, based on the morphological comparisons explicated above proves that the new species is not the same phylogenetic lineage of *P. pollicaris* of Spix.

The 16S rRNA was the most conservative mitochondrial gene used in the delimitation of genetic clusters of *Phyllopezus* (Cacciali *et al.* 2018) and recovered reciprocally monophyletic *P. diamantino* **sp. nov.** and *P. selmae* **sp. nov.** In addition, it was efficient in recovering the phylogenetic relationships of the *Phyllopezus* lineages even among the more recent lineages, as already identified in previous studies (Gamble *et al.* 2012; Cacciali *et al.* 2018).
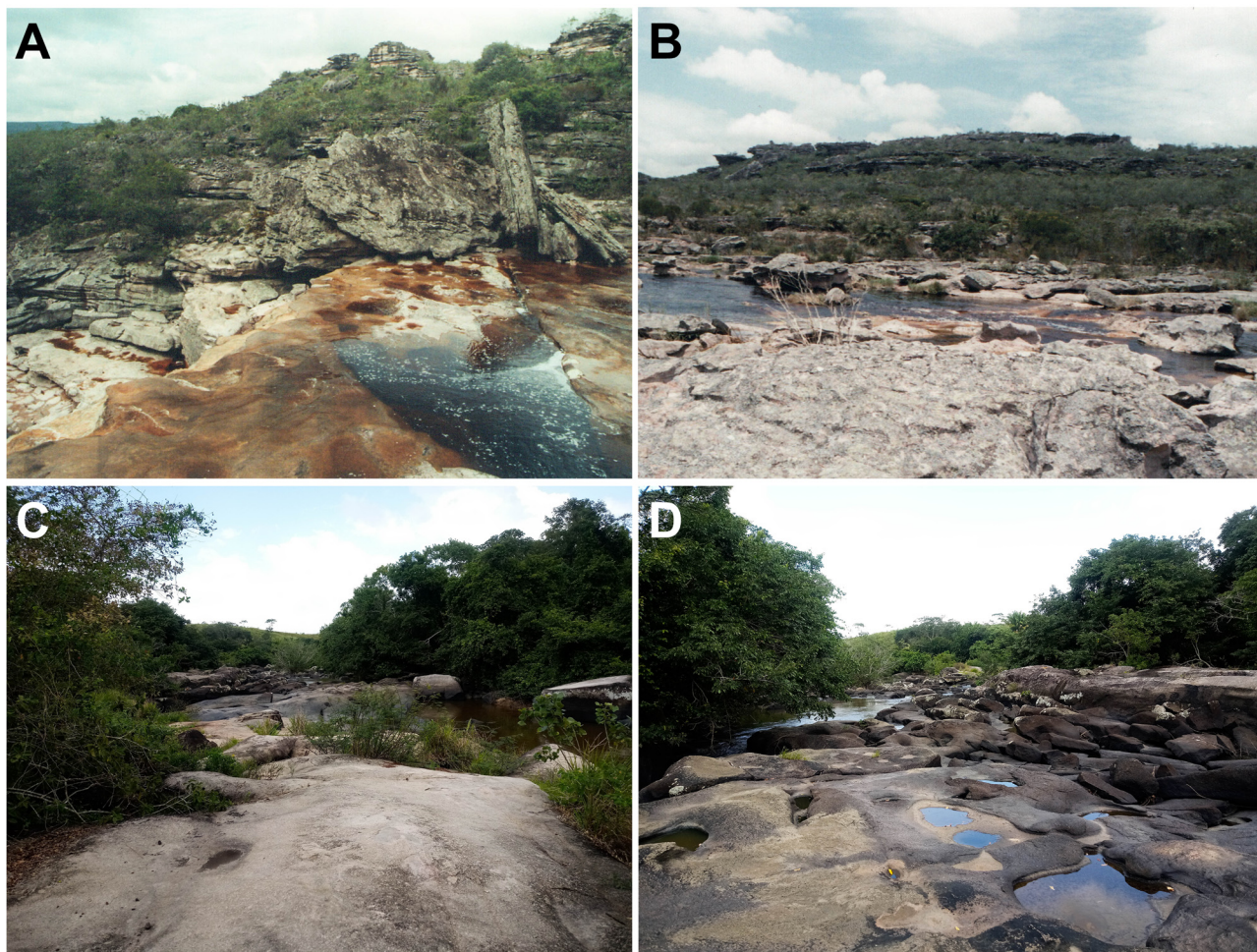

FIGURE 11. Typical environments of the type localities of (A and B) *Phyllopezus diamantino* **sp. nov.** in the municipality of Mucugê, Bahia State and (C and D) *P. selmae* **sp. nov.** in the municipality of Boca da Mata, Alagoas State, Northeastern Brazil.

The high cutoff point for the transition between intra and interspecific variation identified by the analysis of Local Minima (5.73%) and reinforced by ABGD is probably the result of the long and complex evolutionary history of the genus (Werneck *et al.* 2012). According to Werneck *et al.* (2012) the populations of the municipality of Mucugê (Bahia state) (*P. diamantino* **sp. nov.**), together with those of the municipalities of São Geraldo do Araguaia (Pará state) and Barra do Garça (Mato Grosso state) (Clade II; not included in the present study), and now also the lineage of *P. selmae* **sp. nov.** for Alagoas state (*present study*), correspond to the sister clade to all the remaining representatives of the *P. pollicaris* complex. These lineages highly distinct from the other congeners and that diverged earlier (~11.5 Ma). Although related, the lineages within this clade have a widely disjunct distribution and are surrounded by areas of occurrence of other lineages belonging to the complex (Werneck *et al.* 2012). Such

a scenario may represent sampling gaps in some regions or a wide historical extinction of these lineages in the intermediate regions, which may be key to understanding the diversification and current distribution of the oldest lineages of *P. pollicaris* complex.

The type locality of *P. diamantino* **sp. nov.** is located in the northern portion of the *Serra do Espinhaço* mountain range, a region of "*campos rupestres*" with more than 1,000 meters of elevation (Fig. 11A and B). Such mountain regions are characterized by unique floras and a high rate of endemism. Past climates altering and isolating habitats in those mountain ranges may have been related to events that led to the divergence of lineages within the *P. pollicaris* complex. Similar biogeographic scenario has already been reported for frogs (*e.g.*, Lugli & Haddad 2006a, b; Cassimiro *et al.* 2008; Faivovich *et al.* 2009; Pombal Jr *et al.* 2012; Leite *et al.* 2012; Carvalho *et al.* 2013; Trevisan *et al.* 2020), lizards (*e.g.*, Rodrigues *et al.* 2006; Cassimiro & Rodrigues 2009; Rodrigues *et al.* 2009a, b; Rodrigues *et al.* 2017), and amphisbaenians (*e.g.*, Mott *et al.* 2008).

Although Magalhães *et al.* (2015) has not registered any species of *Phyllopezus* during the inventory for the Parque Nacional da Chapada Diamantina, *P. diamantino* **sp. nov.** (identified as *P. pollicaris*) had already been registered for the municipality of Mucugê, state of Bahia (Cassimiro & Rodrigues 2009; Freitas *et al.* 2012). As it is a generally common species where it occurs and of easy observation (MJMD *pers. obs.*) the absence of records in other regions of the park, despite the considerable sampling effort realized by Magalhães et al. (2015) (30 days of sampling effort, 26,640 hours of trap arrays, and 960 hours of active random searches), may be an indication of a restricted distribution of this species. This fact reinforces the need to identify and attribute names to this cryptic species, since the current taxonomic context can give the false impression of a species with wide distribution to lineages that, in fact, are geographically restricted and that may be under different degrees of threat. This fact sometimes hampers the understanding of the evolutionary processes responsible for the pattern of diversification of organisms, in addition to underestimating the degree of threat of a given species, hindering the development of consistent and reliable conservation plans (Meiri *et al.* 2018).

Although *P. selmae* **sp. nov.** is presently know only from state of Alagoas, it is likely that its distribution is underestimated, since the state still has a high level of Wallacean deficit (lack of knowledge of the geographic distribution of species; Whittaker *et al.* 2005). Almost all records for the species are associated with the Coruripe River basin, and the samples were obtained during one of the few herpetofauna inventories carried out in the *Agreste* region of the state, which made the transition between the Atlantic Forest and the semiarid Caatinga biomes (Fig. 11C and D; Gonçalves & Palmeira 2016).

Although we are far from resolving the taxonomy of *P. pollicaris* species complex, the present work is a step forward in that direction formally describing its concealed diversity and unveiling crucial data for conservation policy in a megadiversity but still unknown and so threatened country (Moura & Jetz 2021).

Acknowledgments

References

Albuquerque, P.R.A., Morais, M.D.S.R., Moura, P.T.S., Santos, W.N.S., Costa, R.M.T., Delfim, F.R. & Pontes, B.E.S. (2019) *Phyllopezus lutzae* (Loveridge, 1941) (Squamata, Phyllodactylidae): new records from the Brazilian state of Paraíba. *Check*

List, 15, 49–53.
https://doi.org/10.15560/15.1.49

Brown, S.D., Collins, R.A., Boyer, S., Lefort, M.C., Malumbres-Olarte, J., Vink, C.J. & Cruickshank, R.H. (2012) Spider: an R package for the analysis of species identity and evolution, with particular reference to DNA barcoding. *Molecular Ecology Resources*, 12 (3), 562–565.
https://doi.org/10.1111/j.1755-0998.2011.03108.x

Cacciali, P., Lotzkat, S., Gamble, T. & Koehler, G. (2018) Cryptic Diversity in the Neotropical Gecko Genus *Phyllopezus* Peters, 1878 (Reptilia: Squamata: Phyllodactylidae): A New Species from Paraguay. *International Journal of Zoology*, 2018, 1–14.
https://doi.org/10.1155/2018/3958327

Carvalho, T.R., Leite, F.S.F. & Pezzuti T.L. (2013) A new species of *Leptodactylus* Fitzinger (Anura, Leptodactylidae, Leptodactylinae) from montane rock fields of the Chapada Diamantina, northeastern Brazil. *Zootaxa*, 3701 (3), 349–364.
https://doi.org/10.11646/zootaxa.3701.3.5

Cassimiro, J. & Rodrigues, M.T. (2009) A new species of lizard genus *Gymnodactylus* Spix, 1825 (Squamata: Gekkota: Phyllodactylidae) from Serra do Sincorá, northeastern Brazil, and the status of *G. carvalhoi* Vanzolini, 2005. *Zootaxa*, 2008, 38–52.

Cassimiro, J., Verdade, V.K. & Rodrigues. M.T. (2008) A large and enigmatic new Eleutherodactyline frog (Anura, Strabomantidae) from Serra do Sincorá, Espinhaço range, northeastern Brazil. *Zootaxa*, 1761 (1), 59–68.
https://doi.org/10.11646/zootaxa.1761.1.6

Condez, T.H., Tonini, J.F.R., Pereira-Ribeiro, J. & Dubeux, M.J.M. (2021) On Atlantic Forest rock outcrops: the first record of *Phyllopezus pollicaris* (Spix, 1825) (Squamata, Phyllodactylidae) in the state of Espírito Santo, southeastern Brazil. *Check List*, 17 (5), 1265–1276.
https://doi.org/10.15560/17.5.1265

Faivovich, J., Lugli, L., Lourenço, A.C.C. & Haddad, C.F.B. (2009) A new species of the *Bokermannohyla martinsi* group from central Bahia, Brazil with comments on Bokermannohyla (Anura: Hylidae). *Herpetologica*, 65, 303–310.
https://doi.org/10.1655/0018-0831-65.3.303

Freitas, M.A. & Silva, T.F.S. (2007) *Guia Ilustrado: a herpetofauna das caatingas e áreas de altitudes do nordeste brasileiro*. Editora USEB - União Sul-Americana de Estudos da Biodiversidade, Rio Grande do Sul, 384 pp.

Freitas, M.A., Silva, T. & Loebmann, D. (2012) Squamate Reptiles of the central Chapada Diamantina, with a focus on the municipality of Mucugê, state of Bahia, Brazil. *Check List*, 8, 16–22.
https://doi.org/10.15560/8.1.016

Fujita, M.K., McGuire, J.A., Donnellan, S.C. & Moritz, C. (2010) Diversification and persistence at the arid-monsoonal interface: Australia-wide biogeography of the Bynoe's gecko (*Heteronotia bionoei*: Gekkonidae). *Evolution*, 64, 2293–2314.
https://doi.org/10.1111/j.1558-5646.2010.00993.x

Gamble, T., Colli, G.R., Rodrigues, M.T., Werneck, F.P. & Simons, A.M. (2012) Phylogeny and cryptic diversity in geckos (*Phyllopezus*; Phyllodactylidae; Gekkota) from South America's open biomes. *Molecular Phylogenetics and Evolution*, 62 (3), 943–953.
https://doi.org/10.1016/j.ympev.2011.11.033

Giulietti, A.M. & Pirani, J.R. (1988) Patterns of geographic distribution of some plant species from the Espinhaço range, Minas Gerais and Bahia, Brazil. *In*: Heyer, W.R. & Vanzolini, P.E. (Eds.), *Proceedings of a Workshop on Neotropical Distribution Patterns*. Academia Brasileira de Ciências, Rio de Janeiro, pp. 39–69.

Gonçalves, U. & Palmeira, C.N.S. (2016) Herpetofauna. *In*: Cabral, B.M.A, Neeto, G.G.B. & Daher, M.R.M (Eds.), *Restauração do Rio Coruripe: Um projeto de Resgate Socioambiental*. Gráfica Moura Ramos, Maceió, pp. 36–85.

Katoh, K. & Standley, D.M. (2013) MAFFT multiple sequence alignment software version 7: improvements in performance and usability. *Molecular Biology and Evolution*, 30 (4), 772–780.
https://doi.org/10.1093/molbev/mst010

Kimura, M. (1980) A simple method for estimating evolutionary rates of base substitutions through comparative studies of nucleotide sequences. *Journal of Molecular Evolution*, 16 (2), 111–120.
https://doi.org/10.1007/BF01731581

Koch, C., Venegas, P.J. & Böhme, W. (2006) A remarkable discovery: description of a big-growing new gecko (Squamata: Gekkonidae: *Phyllopezus*) from northwestern Peru. *Salamandra*, 42 (2/3), 145–150.

Köhler, G. (2012) *Color catalogue for field biologists*. Herpeton Verlag, Offenbach, 51pp.

Koslowsky, J. (1895) Un nuevo geco de Matto Grosso. *Revista del Museo de La Plata*, 6 (1894), 371–373.

Kumar, S., Stecher, G., Li, M., Knyaz, C. & Tamura, K. (2018) MEGA X: molecular evolutionary genetics analysis across computing platforms. *Molecular Biology and Evolution*, 35 (6), 1547–1549.
https://doi.org/10.1093/molbev/msy096

Lanfear, R., Calcott, B., Ho, S.Y.W. & Guindon, S. (2012) PartitionFinder: Combined selection of partitioning schemes and substitution models for phylogenetic analyses. *Molecular Biology and Evolution*, 29, 1695–1701.
https://doi.org/10.1093/molbev/mss020

Leite, F.S.F., Pezzuti, T.L. & Garcia, P.C.A. (2012) A new species of the *Bokermanohyla pseudopseudis* group from the Espinhaço Range, central Bahia, Brazil (Anura: Hylidae). *Herpetologica*, 68, 401–409.

https://doi.org/10.1655/HERPETOLOGICA-D-11-00006.1

Lugli, L. & Haddad, C.F.B. (2006a) New species of *Bokermannohyla* (Anura, Hylidae) from central Bahia, Brazil. *Journal of Herpetology*, 40, 7–15.
https://doi.org/10.1670/67-05A.1

Lugli, L. & Haddad, C.F.B. (2006b) A new species of the *Bokermannohyla pseudopseudis* group from central Bahia, Brazil (Amphibia, Hylidae). *Herpetologica*, 62, 453–465.
https://doi.org/10.1655/0018-0831(2006)62[453:ANSOTB]2.0.CO;2

Magalhães, F.M., Laranjeiras, D.O., Costa, T.B., Juncá, F.A., Mesquita, D.O., Röhr, D. L., Silva, W.P., Vieira, G.H.C. & Garda, A.A. (2015) Herpetofauna of protected areas in the Caatinga IV: Chapada Diamantina National Park, Bahia, Brazil. *Herpetology Notes*, 8, 243–261.

Meiri, S., Bauer, A.M., Allison, A., Castro-Herrera, F., Chirio, L., Colli, G., Das, I., Doan, T.M., Glaw, F., Grismer, L.L., Hoogmoed, M., Kraus, F., LeBreton, M., Meirte, D., Nagy, Z.T., Nogueira, C.C., Oliver, P., Pauwels, O.S.G., Pincheira-Donoso, D., Shea, G., Sindaco, R., Tallowin, O.J.S., Torres-Carvajal, O., Trape, J.-F., Uetz, P., Wagner, P., Wang, Y., Ziegler, T. & Roll, U. (2018) Extinct, obscure or imaginary: The lizard species with the smallest ranges. *Diversity and Distributions*, 24 (2), 262–273.
https://doi.org/10.1111/ddi.12678

Moura, M.R. & Jetz, W. (2021) Shortfalls and opportunities in terrestrial vertebrate species discovery. *Nature Ecology & Evolution* 5, 631–639.
https://doi.org/10.1038/s41559-021-01411-5

Mott, T., Rodrigues, M.T., Freitas, M.A. & Silva, T.F.S. (2008) New species of *Amphisbaena* with a nonautotomic and dorsally tuberculate blunt tail from State of Bahia, Brazil (Squamata, Amphisbaenidae). *Journal of Herpetology*, 42 (1), 172–175.
https://doi.org/10.1670/07-074R2.1

Müller, L. & Brongersma, L.D. (1933) Ueber die identität von *Thecadactylus pollicaris* Spix 1825 mit *Phyllopezus goyazensis* Peters 1877. *Zoological Mededelingen*, 15, 156–161.

Palumbi, S., Martin, A., Romano, S., McMilan, W.O., Stice, L. & Grabowski, G. (2002) *The Simple Fool's Guide to PCR*. University of Hawaii, 45 pp.

Pellegrino, K.C.M., Kasahara, S., Rodrigues, M.T. & Yonenaga-Yassuda, Y. (1997) Pericentric inversion events in karyotypic distinction of Brazilian lizards of genus *Phyllopezus* (Squamata, Gekkonidae) detected by chromosomal banding patterns. *Hereditas*, 127 (3), 255–262.
https://doi.org/10.1111/j.1601-5223.1997.t01-1-00255.x

Pombal Jr., J.P., Menezes, V.A., Fontes, A.F., Nunes, I., Rocha, C.D. & Van-Sluys, M. (2012) A second species of the casque-headed frog genus *Corythomantis* (Anura: Hylidae) from northeastern Brazil, the distribution of *C. greeningi*, and comments on the genus. *Boletim do Museu Nacional, Nova Série, Zoologia, Rio de Janeiro*, 530, 1–14.

Pons, J., Barraclough, T.G., Gomez-Zurita, J., Cardoso, A., Duran, D.P., Hazell, S., Kamoun, S., Sumlin, W.D. & Vogler, A.P. (2006) Sequence-based species delimitation for the DNA taxonomy of undescribed insects. *Systematic Biology*, 55, 595–609.
https://doi.org/10.1080/10635150600852011

Puillandre, N., Lambert, A., Brouillet, S. & Achaz, G. (2011) ABGD, automatic barcode gap discovery for primary species delimitation. *Molecular Ecology*, 21, 1864–1877.
https://doi.org/10.1111/j.1365-294X.2011.05239.x

R Core Team (2020) R: a language and environment for statistical computing, version 3.5.0. R Foundation for Statistical Computing, Vienna, Austria. Available from: http://www.r- project.org (accessed 16 Sep 2020)

Reid, N. & Carstens, B. (2012) Phylogenetic estimation error can decrease the accuracy of species delimitation: a Bayesian implementation of the general mixed Yule-coalescent model. *BMC Evolutionary Biology*, 12, 1–11.
https://doi.org/10.1186/1471-2148-12-196

Roberto, I.J, Ávila, R.W. & Melgarejo, A.R. (2015) Répteis (Tesdudines, Squamata, Crocodylia) da Reserva Biológica de Pedra Talhada. *In*: Studer, A., Nusbaumer, L. & Spichiger (Eds.), *Biodiversidade da Reserva Biológica de Pedra Talhada (Alagoas, Pernambuco – Brasil)*. R. Boissiera: mémoires des Conservatoire et Jardin botaniques de la Ville de Genève, Pregny-Chambésy, pp. 357–375.

Rocha, S., Vences, M., Glaw, F., Posada, D. & Harris, D.J. (2009) Multigene phylogeny of Malagasy day geckos of the genus *Phelsuma*. *Molecular Phylogenetics and Evolution*, 52, 530–537.
https://doi.org/10.1016/j.ympev.2009.03.032

Rodrigues, M.T. (1986) Uma nova espécie do gênero Phyllopezus de Cabaceiras: Paraíba: Brasil, com comentários sobre a fauna de lagartos da área (Sauria, Gekkonidae). *Papéis Avulsos de Zoologia*, 36 (20), 237–250.
https://doi.org/10.5962/bhl.part.18420

Rodrigues, M.T., Cassimiro, J., Freitas, M.A. & Silva, T.F.S. (2009a) A new microteiid lizard of the genus *Acratosaura* (Squamata: Gymnophthalmidae) from Serra do Sincorá, State of Bahia, Brazil. *Zootaxa*, 2013, 17–19.
https://doi.org/10.11646/zootaxa.2013.1.2

Rodrigues, M.T., Freitas, M.A. & Silva, T.F.S. (2009b) New species of earless lizard genus *Heterodactylus* (Squamata: Gymnophthalmidae) from the Highlands of Chapada Diamantina, State of Bahia, Brazil. *Journal of Herpetology*, 43 (4), 605–611.

https://doi.org/10.1670/08-133.1

Rodrigues, M.T., Freitas, M.A., Silva, T.F.S. & Bertolotto, C.E.V. (2006) A new species of lizard genus *Enyalius* (Squamata, Leiosauridae) from the highlands of Chapada Diamantina, State of Bahia, Brazil, with a key to species. *Phyllomedusa*, 5 (1), 11–24.
https://doi.org/10.11606/issn.2316-9079.v5i1p11-24

Rodrigues, M.T., Recoder, R., Teixeira Jr, M., Roscito, J.G., Guerrero, A.C., Nunes, P.M.S. & Leite, F.S.F. (2017) A morphological and molecular study of *Psilops*, a replacement name for the Brazilian microteiid lizard genus *Psilophthalmus* Rodrigues 1991 (Squamata, Gymnophthalmidae), with the description of two new species. *Zootaxa*, 4286 (4), 451–482.
https://doi.org/10.11646/zootaxa.4286.4.1

Ronquist, F., Teslenko, M., van der Mark, P., Ayres, D. L., Darling, A., Höhna, S., Larget, B., Liu, L., Suchard, M.A. & Huelsenbeck, J.P. (2012) MrBayes 3.2: efficient bayesian phylogenetic inference and model choice across a large model space. *Systematic Biology*, 61 (3), 539–542.
https://doi.org/10.1093/sysbio/sys029

Sambrook, J. & Russel, D. (2001) *Molecular cloning: a laboratory manual*. Cold Spring. New York, 112 pp.

Spix, J.B. (1825) *Animalia nova sive Species novae lacertarum quas in itinere per Brasiliam annis MDCCCXVII-MDCCCXX jussu et auspicious Maximiliani Josephi I Bavariae Regis suscepto collegit et descripsit Dr. J.B. de Spix*. F.S. Hübschmann, Munich, 26 pp.
https://doi.org/10.5962/bhl.title.5117

Sturaro, M.J., Rodrigues, M.T., Colli, G.R., Knowles, L.L. & Avila-Pires, T.C. (2018) Integrative taxonomy of the lizards *Cercosaura ocellata* species complex (Reptilia: Gymnophthalmidae). *Zoologischer Anzeiger*, 275, 37–65.
https://doi.org/10.1016/j.jcz.2018.04.004

Suchard, M.A., Lemey, P., Baele, G., Ayres, D.L., Drummond, A.J. & Rambaut, A. (2018) Bayesian phylogenetic and phylodynamic data integration using BEAST 1.10. *Virus Evolution*, 4, 1–5.
https://doi.org/10.1093/ve/vey016

Trevisan, C.C., Batalha-Filho, H., Garda, A.A., Menezes, L., Dias, I.R., Solé, M., Canedo, C., Juncá, F.A. & Napoli, M.F. (2020) Cryptic diversity and ancient diversification in the northern Atlantic Forest *Pristimantis* (Amphibia, Anura, Craugastoridae). *Molecular Phylogenetics and Evolution*, 148, 106811.
https://doi.org/10.1016/j.ympev.2020.106811

Vanzolini, P.E. (1953) Sobre o gênero *Phyllopezus* Peters (Sauria, Gekkonidae). *Papéis Avulsos do Departamento de Zoologia*, *Universidade de São Paulo*, 11 (22), 353–369.

Vanzolini, P.E., Ramos-Costa, A.M.M. & Vitt, L.J. (1980) *Répteis das Caatingas*. Academia Brasileira de Ciências. Rio de Janeiro, 161 pp.
https://doi.org/10.5962/bhl.title.109659

Werneck, F.P., Gamble, T., Colli, G.R., Rodrigues, M.T. & Sites, J. (2012) Deep diversification and long-term persistence in the South American "Dry Diagonal": integrating continent-wide phylogeography and distribution modeling of geckos. *Evolution*, 66 (10), 3014–3034.
https://doi.org/10.1111/j.1558-5646.2012.01682.x

Whittaker, R.J., Araújo, M.B., Jepson, P., Ladle, R.J., Watson, J.E.M. & Willis, K.J. (2005) Conservation Biogeography: assessment and prospect. *Diversity and Distributions*, 11, 3–23.
https://doi.org/10.1111/j.1366-9516.2005.00143.x

Zhang, J., Kapli, P., Pavlidis, P. & Stamatakis, A. (2013) A general species delimitation method with applications to phylogenetic placements. *Bioinformatics*, 29 (22), 2869–2876.
https://doi.org/10.1093/bioinformatics/btt499

APPENDIX I. Additional specimens examined

Phyllopezus lutzae: BRAZIL: Paraíba: Pedras de Fogo (CHUFPB 19517, 19518, 19519, 24979); Alagoas: Maceió (UFRN 36, 236; LABI 181, 182, 183); Quebrangulo ([MHNUFAL] = LABI 653).

Phyllopezus periosus: BRAZIL: Paraíba: Cabaceiras (topotypes: CHUFPB 1930, 1931, 1934, 1936, 1939, 1940, 1947); Rio Grande do Norte: Serra Negra do Norte (MHNUFAL 12426, 12428); Currais Novos (UFRN 5551, 5552).

Phyllopezus pollicaris: BRAZIL: Bahia: Paulo Afonso (CHUFPB 11294, 11295, 11296, 11297, 11298, 11299, 11300, 12058, 22330, 25018, 25111, 25137, 25569); Ceará: Aiuaba (CHUFPB 5145, 5147, 5153, 5159, 5160, 5161, 5162, 5163, 5165, 5324, 5325, 5326, 5327, 5328, 5329, 13767, 13768, 13769, 13778, 13780, 13788); Ubajara (CHUFPB 26129, 26894, 26916); Paraíba: Cabaceiras (CHUFPB 10224, 10225, 10228, 10229, 10230, 10231); Pernambuco: Buíque (CHUFPB 23509, 25026, 25562, 25973; [CHUFPE-R] = CAT 272, 391, 271,388, 392); Piauí: Uruçuí (CHUFPB 8697); Floriano (CHUFPB 8699); Coronel José Dias (CHUFPB 14603, 14606, 14608, 14611, 14614, 14616, 14617, 14618); Andorinha (CHUFPB 22324, 22349, 22364, 22450, 22473, 22603); São Raimundo Nonato (CHUFPB 25050, 25153); Sergipe: Canindé de São Francisco (CHUFPB 18559, 18562, 18563, 18567, 18568, 18570, 18573, 18581, 18587, 18592, 18594, 18595, 18602, 18605, 18626, 18633).

APPENDIX II. 16S rRNA mitochondrial gene fragment sequences of *Phyllopezus* samples used in the study. Clades previously delimited by Werneck *et al.* (2012) are identified by Roman numerals.

Species	Clade	Voucher	Locality	GenBank
Phyllopezus diamantino **sp. nov.**	I	(MTR) JC 1185	Mucugê, Bahia, Brazil	JN935553
Phyllopezus diamantino **sp. nov.**	I	(MTR) JC 1219	Mucugê, Bahia, Brazil	JN935554
Phyllopezus selmae **sp. nov.**	-	MHNUFAL 10200	Igaci, Alagoas, Brazil	OM530506
Phyllopezus selmae **sp. nov.**	-	MHNUFAL 13482	Boca da Mata, Alagoas, Brazil	OM530507
Phyllopezus selmae **sp. nov.**	-	MZUSP 106768	Limoeiro de Anadia, Alagoas, Brazil	OM530508
Phyllopezus pollicaris	IV	LG 1309	Serra da Mesa, Goiás, Brazil	JN935569
Phyllopezus pollicaris	IV	LG 1792	Palmas, Tocantins, Brazil	JN935572
Phyllopezus pollicaris	IV	LG 1845	Lajeado, Tocantins, Brazil	JN935574
Phyllopezus pollicaris	VI	MTR 3074	Santo Inácio, Bahia, Brazil	JN935584
Phyllopezus pollicaris	VI	MTR 3287	Santo Inácio, Bahia, Brazil	JN935586
Phyllopezus pollicaris	VI	MTR 3263	Gentio do Ouro, Bahia, Brazil	JN935585
Phyllopezus pollicaris	VII	LG 1310	Niquelândia Goiás, Brazil	JN935568
Phyllopezus pollicaris	VII	CHUNB 36991	Paranã, Tocantins, Brazil	JN935559
Phyllopezus pollicaris	VII	CHUNB 36992	Paranã, Tocantins, Brazil	JN935560
Phyllopezus pollicaris	VII	CHUNB 37001	Paranã, Tocantins, Brazil	JN935561
Phyllopezus pollicaris	VII	CHUNB 43850	São Domingos, Goiás, Brazil	JN935563
Phyllopezus pollicaris	VII	CHUNB 43852	São Domingos, Goiás, Brazil	JN935564
Phyllopezus pollicaris	VIII	MTR 887020	Cabaceiras, Paraíba, Brazil	JN935558
Phyllopezus pollicaris	VIII	LG 1011	Porto Seguro, Bahia, Brazil	JN935566
Phyllopezus pollicaris	VIII	LG 807	Xingó, Alagoas, Brazil	JN935575
Phyllopezus pollicaris	VIII	LG 808	Xingó, Alagoas, Brazil	JN935576
Phyllopezus pollicaris	VIII	LG 1342	Campo Formoso, Bahia, Brazil	JN935570
Phyllopezus pollicaris	VIII	LG 1343	Campo Formoso, Bahia, Brazil	JN935571
Phyllopezus pollicaris	VIII	MTR 2346	Uruçuí-Una, Piauí, Brazil	JN935580
Phyllopezus pollicaris	VIII	MTR 2807	Uruçuí-Una, Piauí, Brazil	JN935581
Phyllopezus pollicaris	VIII	MTR 2958	Uruçuí-Una, Piauí, Brazil	JN935582
Phyllopezus pollicaris	VIII	MTR 2959	Uruçuí-Una, Piauí, Brazil	JN935583

Species	Clade	Voucher	Locality	GenBank
Phyllopezus pollicaris	VIII	MTR 3681	Ilha do Gado Bravo, Bahia, Brazil	JN935587
Phyllopezus pollicaris	VIII	MTR 3748	Alagoado, Bahia, Brazil	JN935588
Phyllopezus pollicaris	VIII	MTR 4960	Serra das Confusões, Piauí, Brazil	JN935589
Phyllopezus pollicaris	VIII	MZUSP 92491	Serra das Confusões, Piauí, Brazil	JN935590
Phyllopezus przewalskii	V	TG 00105	unknown, Paraguay	JN935565
Phyllopezus przewalskii	V	LG 1093	Fuerte Esperanza, Chaco, Argentina	JN935567
Phyllopezus przewalskii	V	MTD 43490	Fortin Toledo, Boqueron, Paraguay	JN935578
Phyllopezus przewalskii	V	MTD 43492	Fortin Toledo, Boqueron, Paraguay	JN935579
Phyllopezus przewalskii	V	MNCN 5903	Serranía Aguarague, Tarija, Bolivia	JN935577
Phyllopezus przewalskii	-	SMF 100495	Paraguay	MF278834
Phyllopezus przewalskii	-	MNHNP 11957	Paraguay	MH397465
Phyllopezus przewalskii	-	MNHNP 11958	Paraguay	MH397466
Phyllopezus heuteri	-	MNHNP 2 39	Cordillera Department, Paraguay	MH397468
Phyllopezus heuteri	-	MNHNP 2 40	Cordillera Department, Paraguay	MH397467
Phyllopezus lutzae	-	CHUNB 50461	Mata de São João, Bahia, Brazil	JN935548
Phyllopezus lutzae	-	CHUNB 50462	Mata de São João, Bahia, Brazil	JN935549
Phyllopezus lutzae	-	CHUNB 50463	Mata de São João, Bahia, Brazil	JN935550
Phyllopezus periosus	-	MTR 887022	Cabaceiras, Paraíba, Brazil	JN935552
Phyllopezus maranjonensis	-	ZFMK 84995	Balsas, Peru	JN935555
Phyllopezus maranjonensis	-	ZFMK 84997	Balsas, Peru	JN935557
Phyllopezus maranjonensis	-	ZFMK 84996	Balsas, Peru	JN935556
Phyllodactylus xanti	-	ROM 38490	Baja California Sur, Mexico	AY763284

APPENDIX III. Morphometrics (in mm) and meristic data [mean ± standard deviation (range)] of *Phyllopezus* occurring in northeastern Brazil. Details of acronyms of characteristics are mentioned in "Material and methods" section.

	P. lutzae		*P. periosus*		*P. pollicaris* sensu lato	
	Male(n = 3)	Female(n = 7)	Male(n = 10)	Female(n = 4)	Male(n = 43)	Female(n = 44)
SVL	61 ±1.61 (59.61—62.77)	56.93 ±2.85 (53.2—60)	107.23 ±4.27 (101.34—113.62)	104.03 ±4.21 (97.28—108.38)	73.31 ±4.94 (65.12—85.6)	70.78 ±4.96 (63.65—87.11)
DBL	26.12 ±1.1 (25.36—27.38)	24.06 ±1.92 (20.94—26.2)	46.3 ±2.91 (41.56—50.43)	45.68 ±2.26 (42.1—47.69)	31.7 ±2.42 (28.53—38.8)	30.75 ±2.84 (25.51—37.37)
TBW	6.95 ±0.44 (6.58—7.44)	6.91 ±1.81 (5.35—10.84)	13.36 ±1.43 (11.63—15.43)	10.45 ±1.94 (8.36—13.64)	9.03 ±1.41 (7.27—13.07)	8.49 ±1.18 (5.5—11.58)
HL	17.58 ±0.67 (16.99—18.3)	14.9 ±3.41 (7.35—17.49)	29.98 ±1.65 (27—32.4)	30 ±1.52 (27.38—31.21)	20.67 ±1.41 (18.49—25.3)	19.79 ±1.44 (17.42—23.46)
HW	11.6 ±0.45 (11.1—11.96)	11.76 ±2.26 (10.31—16.76)	22 ±1.17 (19.81—23.67)	21.09 ±1.46 (19—23.11)	15.32 ±1.04 (13.61—18.3)	14.25 ±1.11 (12.32—17.46)
HD	6.1 ±0.43 (5.83—6.59)	5.76 ±0.65 (4.63—6.72)	12.55 ±1.12 (11.28—14.2)	12.51 ±1.18 (11.38—13.8)	8.19 ±0.9 (6.22—10.43)	7.95 ±0.86 (6.36—9.65)
SL	7.33 ±0.13 (7.2—7.45)	6.96 ±0.34 (6.32—7.37)	12.84 ±0.62 (11.68—13.83)	12.75 ±0.38 (12.1—13.08)	8.24 ±0.59 (7.17—10.32)	7.87 ±0.59 (6.99—9.33)
NSD	1.65 ±0.22 (1.39—1.79)	1.7 ±0.17 (1.46—1.96)	2.48 ±0.4 (2—3.22)	2.94 ±0.24 (2.74—3.3)	1.94 ±0.31 (1.4—3.08)	1.77 ±0.25 (1.25—2.29)

	P. lutzae		*P. periosus*		*P. pollicaris* sensu lato	
	Male(n = 3)	Female(n = 7)	Male(n = 10)	Female(n = 4)	Male(n = 43)	Female(n = 44)
ESD	5.43 ±0.2	5.34 ±0.44	10.32 ±0.66	9.79 ±0.64	6.48 ±0.41	6.23 ±0.58
	(5.2—5.59)	(4.57—5.78)	(8.87—10.89)	(8.67—10.24)	(5.53—7.49)	(5.25—7.79)
ED	3.34 ±0.22	3.27 ±0.29	6.09 ±0.45	6.06 ±0.26	4.36 ±0.41	4.27 ±0.36
	(3.09—3.49)	(2.92—3.54)	(5.4—6.66)	(5.66—6.35)	(3.52—5.46)	(3.29—5.32)
IOD	5.91 ±0.3	5.44 ±0.66	9.9 ±0.53	8.95 ±0.21	7.2 ±0.66	6.86 ±0.61
	(5.62—6.21)	(4.78—6.78)	(9.17—10.84)	(8.68—9.17)	(5.56—8.41)	(5.84—8.73)
IND	2.48 ±0.07	2.2 ±0.18	3.87 ±0.49	3.81 ±0.16	2.69 ±0.3	2.61 ±0.29
	(2.4—2.54)	(1.94—2.38)	(3.34—4.88)	(3.71—4.09)	(2—3.46)	(1.98—3.32)
LH	11.49 ±0.8	10.76 ±0.57	23.26 ±1.94	20.09 ±0.86	15.09 ±1.27	14.43 ±1.33
	(10.58—12.06)	(9.99—11.71)	(21.22—26.73)	(19.26—21.46)	(13.12—18.03)	(11.8—18.37)
LF	7.09 ±0.44	6.84 ±0.39	14.82 ±0.6	14.18 ±0.69	9.65 ±0.78	9.07 ±0.72
	(6.59—7.4)	(6.12—7.41)	(13.92—15.78)	(13.27—15.09)	(7.59—11.29)	(7.76—11)
LT	12.24 ±0.51	11.91 ±0.34	25.68 ±1.06	25.39 ±1.61	16.12 ±1.25	15.54 ±1.23
	(11.69—12.7)	(11.49—12.39)	(24.26—27.75)	(23.04—27.15)	(13.79—19.76)	(13.08—18.13)
LTB	8.51 ±0.18	8.18 ±0.48	18.63 ±1.15	17.67 ±0.84	11.58 ±0.9	11.05 ±0.8
	(8.31—8.63)	(7.27—8.7)	(15.73—19.86)	(16.51—18.48)	(10.23—14.3)	(9.51—13.12)
WM	2.46 ±0.02	2.32 ±0.21	5.09 ±1.61	4.54 ±0.26	3.08 ±0.32	2.93 ±0.26
	(2.44—2.48)	(2.06—2.67)	(3.85—8.8)	(4.21—4.85)	(2.49—4.14)	(2.27—3.58)
LM	1.19 ±0.15	0.96 ±0.11	2.49 ±0.45	2.16 ±0.27	1.56 ±0.19	1.48 ±0.18
	(1.03—1.32)	(0.8—1.17)	(1.84—3.2)	(1.79—2.48)	(1.15—1.93)	(1.15—1.95)
WR	2.68 ±0.05	2.48 ±0.32	4.69 ±0.36	4.63 ±0.26	3.3 ±0.28	3.08 ±0.33
	(2.64—2.74)	(2.06—2.96)	(4.26—5.28)	(4.35—4.96)	(2.83—4.12)	(2.1—3.92)
LR	1.55 ±0.16	1.64 ±0.22	6.34 ±0.44	6.28 ±0.54	3.47 ±0.43	3.33 ±0.48
	(1.37—1.66)	(1.33—1.97)	(5.36—6.81)	(5.74—7.19)	(2.54—4.27)	(2.53—4.8)
R	1 ±0(1—1)	1 ±0(1—1)	1 ±0(1—1)	1 ±0(1—1)	1 ±0(1—1)	1 ±0(1—1)
PR	3 ±1(2—3)	3 ±0(2—3)	2 ±0(2—2)	2 ±0(2—2)	2 ±0(2—3)	2 ±0(2—3)
PN	2 ±0(2—2)	2 ±0(2—3)	3 ±1(2—3)	2 ±1(2—3)	2 ±0(2—2)	2 ±0(2—2)
SL	8 ±1(8—9)	8 ±1(8—9)	8 ±1(7—9)	7 ±0(7—7)	7 ±0(6—8)	7 ±0(6—8)
IL	7 ±1(7—8)	7 ±1(7—8)	7 ±1(6—8)	6 ±1(6—7)	6 ±0(5—7)	6 ±0(6—7)
VLR	59 ±4(56—63)	60 ±3(56—64)	43 ±3(38—48)	44 ±1(42—46)	47 ±4(40—60)	45 ±3(39—55)
DT	31 ±11(20—42)	33 ±8(20—43)	45 ±4(37—49)	43 ±4(40—50)	38 ±4(34—47)	37 ±4(30—49)
L4F	10 ±1(9—10)	10 ±1(9—11)	14 ±1(13—15)	13 ±1(12—14)	11 ±1(10—14)	11 ±1(10—14)
L4T	11 ±2(9—12)	11 ±1(9—12)	14 ±1(13—16)	14 ±0(13—14)	12 ±1(10—13)	11 ±1(10—13)
TP	0 ±0(0—0)	0 ±0(0—0)	2 ±1(2—3)	2 ±1(1—2)	3 ±1(0—5)	2 ±1(0—4)
CP	0 ±1(0—1)	0 ±1(0—1)	1 ±0(1—1)	1 ±0(1—1)	0 ±0(0—1)	0 ±1(0—1)

	Phyllopezus diamantino sp. nov.		*Phyllopezus selmae* sp. nov.	
	Male(n = 5)	Female(n = 6)	Male(n = 9)	Female(n = 13)
SVL	84.66 ±6.7	76.67 ±4	93.59 ±3.68	92.06 ±5.61
	(76.41—96.25)	(72.38—82.36)	(89.2—100.24)	(83.5—99.47)
DBL	35.55 ±2.87	31.45 ±2.44	41.28 ±1.35	40.53 ±1.49
	(32.07—39.06)	(28.09—34.07)	(38.6—43.05)	(38.61—42.82)

	Phyllopezus diamantino sp. nov.		*Phyllopezus selmae* sp. nov.	
	Male(n = 5)	Female(n = 6)	Male(n = 9)	Female(n = 13)
TBW	8.46 ±1.2	6.87 ±0.47	11.2 ±0.58	9.91 ±1.08
	(6.56─10.12)	(6.36─7.49)	(10.34─11.91)	(9.02─12.31)
HL	24.1 ±2.05	22.12 ±1.1	25.22 ±0.59	24.87 ±1.37
	(21.46─27.75)	(21.08─23.93)	(24.41─26.21)	(22.88─27.02)
HW	16.45 ±1.84	14.29 ±0.73	18.33 ±0.94	17.72 ±0.97
	(13.47─19.17)	(13.16─14.89)	(17.4─20.23)	(16.18─19.53)
HD	8.07 ±0.73	7.22 ±0.4	9.86 ±0.82	8.62 ±0.66
	(7.3─9.06)	(6.55─7.55)	(8.89─10.97)	(7.47─9.54)
SL	9.98 ±0.71	8.98 ±0.46	10.22 ±0.44	10.15 ±0.49
	(8.93─11.01)	(8.5─9.69)	(9.68─10.99)	(9.48─11.08)
NSD	2.08 ±0.19	1.92 ±0.08	2.28 ±0.2	2.27 ±0.37
	(1.9─2.42)	(1.83─2.02)	(1.95─2.53)	(1.75─2.75)
ESD	7.76 ±0.72	6.99 ±0.29	7.71 ±0.53	7.79 ±0.35
	(6.76─8.82)	(6.75─7.32)	(6.94─8.41)	(7.38─8.29)
ED	5.24 ±1.11	4.66 ±0.52	5.08 ±0.3	5.19 ±0.49
	(3.72─6.94)	(4.11─5.16)	(4.56─5.39)	(4.76─6.09)
IOD	7.48 ±0.79	6.39 ±0.7	8.58 ±0.63	8.34 ±0.51
	(6.65─8.87)	(5.65─7.08)	(7.55─9.28)	(7.73─9.39)
IND	2.98 ±0.35	2.77 ±0.31	3.37 ±0.32	3.27 ±0.28
	(2.64─3.38)	(2.47─3.24)	(3.12─3.98)	(2.77─3.79)
LH	18.07 ±1.64	16.11 ±0.51	18.38 ±1.44	18.54 ±0.88
	(16.37─21.04)	(15.65─16.72)	(17.04─20.84)	(17.36─20.11)
LF	11.89 ±0.72	10.94 ±0.48	11.75 ±0.71	11.28 ±0.57
	(10.91─13.13)	(10.35─11.36)	(10.67─12.81)	(10.34─12.23)
LT	20.24 ±1.24	18.44 ±1.06	21.02 ±1.78	19.97 ±1.21
	(18.32─22.02)	(17.28─19.58)	(19.25─24.12)	(18.06─21.23)
LTB	14.06 ±0.91	13.1 ±0.72	14.46 ±0.7	14.07 ±0.73
	(12.57─15.41)	(12.16─13.94)	(13.51─15.4)	(13.04─15.3)
WM	3.76 ±0.21	3.43 ±0.24	3.87 ±0.3	4.03 ±0.38
	(3.56─4.05)	(3.14─3.76)	(3.39─4.23)	(3.54─4.54)
LM	1.93 ±0.19	1.58 ±0.18	2.11 ±0.2	2.02 ±0.23
	(1.6─2.16)	(1.39─1.85)	(1.82─2.33)	(1.52─2.3)
WR	4.38 ±0.41	3.74 ±0.44	4.03 ±0.19	4.26 ±0.37
	(3.65─4.77)	(3.13─4.23)	(3.82─4.32)	(3.53─4.64)
LR	4.07 ±0.32	3.34 ±0.36	4.03 ±0.38	4.15 ±0.46
	(3.67─4.58)	(2.82─3.74)	(3.51─4.46)	(3.57─4.98)
R	1 ±0(1─1)	1 ±0(1─1)	1 ±0(1─1)	1 ±0(1─1)
PR	2 ±1(2─3)	2 ±0(2─2)	2 ±0(2─2)	2 ±0(2─2)
PN	2 ±0(2─2)	2 ±0(2─2)	2 ±0(2─3)	2 ±0(2─2)
SL	7 ±0(6─7)	7 ±0(7─7)	7 ±0(6─7)	7 ±0(7─8)
IL	7 ±0(6─7)	7 ±1(6─7)	6 ±1(6─7)	7 ±0(6─7)
VLR	56 ±3(51─59)	55 ±2(52─57)	46 ±1(44─48)	46 ±2(45─51)
DT	45 ±5(38─52)	47 ±3(43─50)	45 ±2(41─47)	44 ±1(42─46)
L4F	12 ±1(11─13)	12 ±1(11─13)	13 ±1(12─14)	13 ±1(11─14)

	Phyllopezus diamantino sp. nov.		*Phyllopezus selmae* sp. nov.	
	Male(n = 5)	Female(n = 6)	Male(n = 9)	Female(n = 13)
L4T	13 ±1(12—14)	13 ±1(12—14)	14 ±1(13—15)	13 ±1(12—14)
TP	2 ±0(2—3)	2 ±0(2—2)	2 ±0(2—3)	2 ±1(0—3)
CP	1 ±0(1—1)	1 ±0(1—1)	0 ±0(0—0)	0 ±0(0—0)